mathematics

MDPI

Article

Seasonal Mathematical Model of Salmonellosis Transmission and the Role of Contaminated Environments and Food Products

Mohammed H. Alharbi [1,*,†], Fawaz K. Alalhareth [2,†] and Mahmoud A. Ibrahim [3,4,5,*,†]

[1] Department of Mathematics and Statistics, College of Science, University of Jeddah, Jeddah 21589, Saudi Arabia
[2] Department of Mathematics, College of Arts and Sciences, Najran University, Najran 55461, Saudi Arabia
[3] Bolyai Institute, University of Szeged, Aradi vértanúk tere 1., 6720 Szeged, Hungary
[4] National Laboratory for Health Security, University of Szeged, Aradi vértanúk tere 1., 6720 Szeged, Hungary
[5] Department of Mathematics, Faculty of Science, Mansoura University, Mansoura 35516, Egypt
* Correspondence: mhhalharbi1@uj.edu.sa (M.H.A.); mibrahim@math.u-szeged.hu or mahmoud_ali@mans.edu.eg (M.A.I.)
† These authors contributed equally to this work.

Abstract: Salmonellosis continues to be a global public health priority in which humans, livestock, and the contaminated environment interact with food to create complex interactions. Here, a new non-autonomous model is proposed to capture seasonal dynamics of Salmonella typhimurium transmission with key compartments that include humans, cattle, and bacteria in environmental and food sources. The model explores how bacterial growth, shedding, and ingestion rates, along with contamination pathways, determine disease dynamics. Some analytical derivations of the basic reproduction number ($\mathcal{R}_0$) and threshold conditions for disease persistence or extinction are derived by using the spectral radius of a linear operator associated with the monodromy matrix. Parameter estimation for the model was accomplished with the aid of Latin hypercube sampling and least squares methods on Salmonella outbreak data from Saudi Arabia ranging from 2018 to 2021. The model was able to conduct an analysis based on the estimated 0.606 value of $\mathcal{R}_0$, and this meant that the model was able to fit reasonably well for both the cumulative and the new individual case data, which in turn, suggests the disease is curable. Predictions indicate a gradual decline in the number of new cases, with stabilization anticipated at approximately 40,000 cumulative cases. Further simulations examined the dynamics of disease extinction and persistence based on $\mathcal{R}_0$. When $\mathcal{R}_0$ is less than 1, the disease-free equilibrium is stable, resulting in the extinction of the disease. Conversely, when $\mathcal{R}_0$ exceeds 1, the disease persists, exhibiting endemic characteristics with recurrent outbreaks. Sensitivity analysis identified several parameters as having a significant impact on the model's outcomes, specifically mortality and infection rates, along with decay rates. These findings highlight the critical importance of precise parameter estimation in understanding and controlling the transmission dynamics of Salmonella. Sensitivity indices and contour plots were employed to assess the impact of various parameters on the basic reproduction number and provide insights into the factors most influencing disease transmission.

Keywords: Salmonella typhimurium; non-autonomous model; basic reproduction number ($\mathcal{R}_0$); seasonal dynamics; sensitivity analysis; global stability; periodic solutions

MSC: 34A99; 34C25; 34C60; 92D30

check for updates

Academic Editor: Takashi Suzuki

Received: 25 December 2024
Revised: 14 January 2025
Accepted: 18 January 2025
Published: 20 January 2025

Citation: Alharbi, M.H.; Alalhareth, F.K.; Ibrahim, M.A. Seasonal Mathematical Model of Salmonellosis Transmission and the Role of Contaminated Environments and Food Products. *Mathematics* **2025**, *13*, 322. https://doi.org/10.3390/math13020322

Copyright: © 2025 by the authors. Licensee MDPI, Basel, Switzerland. This article is an open access article distributed under the terms and conditions of the Creative Commons Attribution (CC BY) license (https://creativecommons.org/licenses/by/4.0/).

1. Introduction

Salmonellosis is a major global public health threat, contributing significantly to morbidity, mortality, and economic hardship. This foodborne and zoonotic disease is caused by the ingestion of Salmonella typhimurium bacteria, which can contaminate food, water, and the environment [1]. The primary sources of infection include dairy products, fruits, vegetables, and contact with infected animals or contaminated surfaces [1,2]. Salmonellosis symptoms in humans include diarrhea, vomiting, abdominal pain, fever, and headaches, which typically appear a few hours to a few days after infection. While most cases resolve without treatment, severe infections may require hospitalization or antibiotic intervention. In cattle, salmonellosis causes severe diarrhea, fever, and dehydration, with infected cattle shedding bacteria into the environment. This can lead to a cycle of reinfection and contamination of dairy products, posing a risk to animal health and human consumers [3]. Salmonellosis is responsible for approximately 93.8 million human infections and 150,000 deaths annually, burdening healthcare systems and affecting economic productivity [4–7].

Seasonality, characterized by fluctuations in disease cases corresponding to specific calendar periods, is a common feature of many public health-related diseases, including Salmonella. Salmonella thrives at temperatures between 7.5 °C and 37 °C, with optimal growth at 35–37 °C, conditions similar to those found in the host's intestines [8,9]. Haley et al. [10] found that Salmonella levels in surface waters were significantly higher in summer, correlating with rainfall and water temperature, with peak serotype diversity in August. Similarly, ref. [11] observed higher Salmonella prevalence in Ethiopian dairy products during the dry season, particularly in raw milk, highlighting the influence of seasonal factors on contamination. Bondo et al. [12] linked Salmonella in raccoon feces to rainfall and season, suggesting raccoons as potential carriers in various environments. Environmental and wildlife factors also play a significant role in Salmonella persistence and transmission. Martínez-Urtaza and Liébana [13] identified persistent Salmonella Senftenberg strains in marine environments, tied to mussel-processing facilities, emphasizing the role of environmental reservoirs. Oludairo et al. [14] noted that wild animals, including reptiles and rodents, serve as asymptomatic carriers, maintaining Salmonella in the environment. Roshdy et al. [15] observed higher Salmonella infection rates in broiler chicks during summer, with antibiotic resistance genes posing additional public health risks. These findings underscore the complex interplay of seasonality, environmental reservoirs, and wildlife in Salmonella epidemiology.

Unlike other foodborne diseases, salmonellosis is a zoonotic infection affecting humans and animals, particularly cattle. Infected cattle shed Salmonella bacteria into the environment through fecal excretion, where the bacteria persist under favorable conditions, such as warm temperatures, alkaline pH, and moisture. These contaminated environments can then infect both humans and cattle, creating a cycle of reinfection. The bacteria's survival and proliferation in the environment exacerbate the risk of cross-contamination, especially in crowded dairy farms, food processing facilities, and restaurants where hygiene protocols are poorly observed [16].

As salmonellosis continues to pose a significant health and economic burden worldwide, particularly in dairy-producing regions, mathematical epidemiology offers a comprehensive framework for predicting outbreaks, guiding control measures, and minimizing its impact on public health systems. Qin et al. [17] developed a novel epidemiological model for Salmonella infections by integrating environmental risk factors with traditional SIR (susceptible–infected–recovery) models. Their model used person-to-person transmission and environmental factors, including seasonal temperature variations, to predict infection rates. Simulations based on Canadian data from 1996 to 2002 showed that the

model, especially its improved version considering seasonal effects, aligned well with observed infection trends. They concluded that incorporating temperature and other risk factors significantly enhances the prediction accuracy compared to standard models. Collineau et al. [18] developed a within-flock SEIR model to simulate the transmission dynamics of Salmonella Heidelberg in Canadian broiler chicken flocks. The model assessed the within-flock prevalence and environmental bacterial concentrations, exploring various intervention strategies, including vaccination and cleaning protocols. Results showed that broiler chicken flock vaccination significantly reduced bacterial concentrations while cleaning and disinfection effectively decreased within-flock prevalence. However, extended downtime between flocks had minimal impact, highlighting the importance of integrated control measures for managing Salmonella Heidelberg. Trazias et al. [19] proposed a comprehensive non-linear ODE-based epidemiological model to investigate the transmission dynamics of salmonellosis in human and dairy cattle populations. The model incorporates eight compartments, including human and cattle populations, as well as environmental and dairy product contamination. Using parameter estimation from data spanning 1990 to 2020, they identified key factors such as bacterial shedding, ingestion rates, and bacterial decay rates as critical to the disease's persistence. Their analysis revealed that increasing shedding rates and bacterial survival in the environment significantly increased the basic number of reproduction, $\mathcal{R}_0$, highlighting the need for interventions, such as hygiene practices, thorough cooking of food, and isolation of infected cattle, to reduce salmonellosis transmission. Nyerere et al. [20] constructed a deterministic model for brucellosis that integrates seasonality into the transmission parameters affecting domestic ruminants, wild animals, humans, and the environment. The study's findings underscored the significant impact of seasonal weather variations on the transmission dynamics of brucellosis. It emphasized the necessity for the timely implementation of control measures to mitigate the disease during periods characterized by fluctuating transmission rates. Naumova et al. [21] established a framework to evaluate disease seasonality, examining six enterically transmitted diseases (EDs) in Massachusetts over a period of 10 years. All EDs, with the exception of hepatitis A, exhibited distinct seasonal patterns. Specifically, Campylobacter and Salmonella peaked 2–14 days following temperature peaks, whereas Cryptosporidium, Shigella, and Giardia demonstrated lags of $>$40 days. This methodology offered comprehensive quantification of seasonality, which is instrumental for disease surveillance and enhancing the comprehension of environmental influences on transmission. Other studies have also investigated the impacts of seasonality and environmental factors on foodborne diseases [22,23].

This study aims to investigate the seasonal dynamics of Salmonella Typhimurium transmission within human, cattle, and environmental compartments, focusing on the impacts of seasonal variations, contamination through food products, and key parameters that influence disease transmission. Consequently, we propose a non-autonomous mathematical model to examine the transmission dynamics of Salmonella under conditions of periodic environmental variability. We derive the basic reproduction number $\mathcal{R}_0$ for the periodic model to illustrate both global stability and the existence of positive periodic solutions, which depend on the parameter value of $\mathcal{R}_0$. Our primary objective is to use our model to analyze the dynamics of salmonella transmission during the outbreak in Saudi Arabia from 2018 to 2021. We calibrate the model using empirical data from Saudi Arabia and estimate various parameters. Subsequently, a sensitivity analysis is performed to identify the parameters that significantly affect the transmission of diseases within the human population. This analysis involves the calculation of sensitivity indices and the impacts of environments and contaminated food products. In addition, we provide numerical simulations to validate and substantiate the analytical results.

The article is structured to present the modeling, analysis, and applications of the proposed Salmonellosis epidemiological model. Section 2 outlines the model development, assumptions, and key properties. Section 3 derives the basic reproduction number ($\mathcal{R}_0$) of the non-autonomous system, which will be used to demonstrate either the extinction or persistence of the disease. Section 4 investigates the stability of disease-free equilibrium and the existence of endemic periodic solutions. Section 5 presents computational experiments, model calibration using data from the 2018–2021 Salmonella outbreak in Saudi Arabia, and sensitivity analysis. The section concludes with a predictive model for future Salmonella cases.

2. Model Formulation

This work develops a seasonal mathematical model that describes the dynamics of Salmonella Typhimurium, considering interactions between human and cattle populations and bacterial concentrations in environments and food. The framework incorporates nine key compartments: S_h (susceptible humans), I_h (infected humans), R_h (recovered humans), I_c (infected cattle), S_c (susceptible cattle), E_c (exposed cattle), R_c (recovered cattle), B (bacterial concentration in environments), and F (bacterial concentration in food products). Consequently, the total populations of humans and cattle over time are determined by

$$\begin{aligned} N_h(t) &= S_h(t) + I_h(t) + R_h(t), \\ N_c(t) &= S_c(t) + E_c(t) + I_c(t) + R_c(t). \end{aligned}$$

Figure 1 provides a visual depiction of the model.

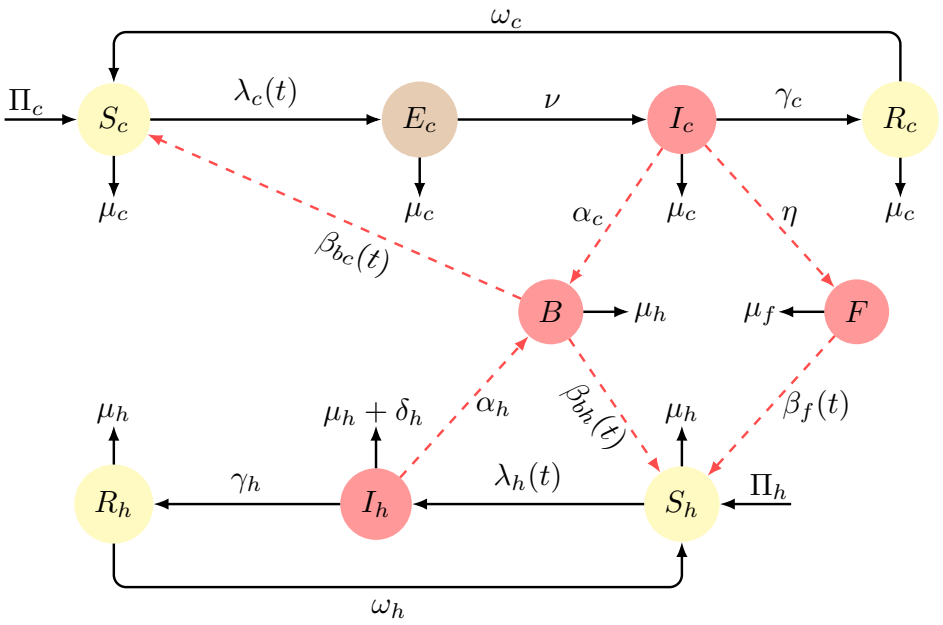

Figure 1. Diagram illustrating the flow of the model (1).

The model equations can be expressed, utilizing the previously established notations and referring to Figure 1, as follows:

$$\begin{aligned} S_h'(t) &= \Pi_h - \lambda_h(t)S_h(t) - \mu_h S_h(t) + \omega_h R_h(t), \\ I_h'(t) &= \lambda_h(t)S_h(t) - \gamma_h I_h(t) - (\delta_h + \mu_h)I_h(t), \\ R_h'(t) &= \gamma_h I_h(t) - \mu_h R_h(t) - \omega_h R_h(t), \\ S_c'(t) &= \Pi_c - \lambda_c(t)S_c(t) - \mu_c S_c(t) + \omega_c R_c(t), \end{aligned}$$

$$
\begin{aligned}
E_c^{'}(t) &= \lambda_c(t)S_c(t) - \nu E_c(t) - \mu_c E_c(t), \\
I_c^{'}(t) &= \nu E_c(t) - \gamma_c I_c(t) - (\delta_c + \mu_c) I_c(t), \\
R_c^{'}(t) &= \gamma_c I_c(t) - \mu_c R_c(t) - \omega_c R_c(t), \\
B^{'}(t) &= \alpha_h I_h(t) + \alpha_c I_c(t) - \mu_b B(t), \\
F^{'}(t) &= \eta I_c(t) - \mu_f F(t),
\end{aligned} \tag{1}
$$

where

$$
\begin{aligned}
\lambda_h(t) &= \beta_h I_h(t) + \beta_{bh}(t)B(t) + \beta_f(t)F(t), \\
\lambda_c(t) &= \beta_c I_c(t) + \beta_{bc}(t)B(t).
\end{aligned}
$$

Given the short incubation period of Salmonella typhimurium in humans, the exposed human compartment is omitted from the model to simplify its structure [2]. The symbols Π_h and μ_h denote the recruitment rate of humans and the natural death rate, respectively. Upon infection, susceptible individuals transition to the infected class (I_h), where they remain for a specified duration $1/\gamma_h$ before recovery or may succumb to disease-induced mortality at a rate of δ_h. The force of infection within the human population, denoted by $\lambda_h(t)$, can occur through various transmission pathways, including human-to-human transmission at a rate β_h, environment-to-human transmission at a rate $\beta_{bh}(t)$, or transmission through contaminated food products at a rate $\beta_f(t)$. Recovery after infection gradually loses immunity at a rate of ω_h. Π_c and μ_c are used to denote the recruitment rate of cattle and their natural mortality rate, respectively. Upon infection, susceptible cattle move to the exposed class (E_c), where the infection rate for these cattle is represented by $\lambda_c(t)$. This infection can be transmitted through the interaction among cattle at a rate β_c or environmental exposure at a rate $\beta_{bc}(t)$. Cattle in the exposed E_c class progress to symptomatic infection (I_c) at a rate determined by ν. Those cattle that are symptomatic and infectious recover subsequently at a steady rate as indicated by γ_c. Recovery after infection gradually loses immunity at a rate of ω_c.

The model assumes homogeneous mixing, suggesting that each individual has an equal probability of contacting any other individual, as determined by the infection terms ($\lambda_h(t)$ and $\lambda_c(t)$). Despite being a useful abstraction of the population contact structure, this assumption may not accurately reflect reality. We also consider population sizes to be constant taking into account population recruitment Π_h, Π_c and natural death rates μ_h, μ_c. This approach allows the model to concentrate on the relative proportions of individuals in various states, which is a valid simplification when the dynamics of disease occur over a much shorter time scale than that of demographic processes. Although these assumptions may not be universal, they provide a fundamental framework from which to comprehend the basic dynamics of disease transmission. In our model, the transmission rates of Salmonella infections from environmental and food sources to humans and cattle are represented by $\beta_{bh}(t)$, $\beta_{bc}(t)$, and $\beta_f(t)$. These functions are defined as continuous positive functions with a period P, designed to account for seasonal fluctuations in disease spread, as described in Equation (1). This phenomenon reflects the observed seasonality in Salmonella infections, which are influenced by various factors, including temperature, rainfall, and human behavioral patterns. A detailed summary of the model parameters is presented in Table 1 for better understanding.

Table 1. The parameters of Model (1), alongside a comprehensive description.

Parameters	Description
Π_h, μ_h	Human recruitment and death rates
β_h	Human infection rate from infected to susceptible
$\beta_{bh}(t)$	Rate of infection from environment to susceptible human
$\beta_f(t)$	Food product-to-susceptible human infection rate
$1/\delta_h$	Duration of human infectiousness
$1/\omega_h$	Duration of temporary full immunity to infection in humans
γ_h	Human recovery rate
Π_c, μ_c	Cattle birth and mortality rates
β_c	Rate of infection from infected to susceptible cattle
$\beta_{bc}(t)$	Rate of infection from environment to susceptible cattle
ν	Rate of progression to infected cattle
$1/\delta_c$	Duration of infectiousness
γ_c	Cattle recovery rate
$1/\omega_c$	Duration of temporary full immunity to infection in cattle
α_h	Bacteria shedding rate of infected human
α_c	Bacteria shedding rate of infected cattle
μ_b	Bacteria in the environment decay rate
η	Bacteria in food product excretion
μ_f	Bacteria in food product decay rate

Basic Properties

To begin with, our objective is to investigate whether solutions to Model (1) exist and are unique. In order to streamline this analysis, we will first define some useful notations.

$$\phi(0) = \big(S_h(0), I_h(0), R_h(0), S_c(0), E_c(0), I_c(0), R_c(0), B(0), F(0)\big) \in \mathbb{R}^9_+,$$

where $\mathbb{R}_+$ denotes the set of non-negative real numbers. Based on Theorem 5.2.1 from [24], it follows that the Cauchy problem for Model (1) has a unique non-negative local solution

$$\big(S_h(t), I_h(t), R_h(t), S_c(t), E_c(t), I_c(t), R_c(t), B(t), F(t)\big),$$

for any initial value $\phi(0) \in \mathbb{R}^9_+$. Given an initial positive condition, consider the human subsystem described by (1), let

$$N_h(t) = S_h(t) + I_h(t) + R_h(t).$$

Then, $N(t)$ satisfies

$$N_h'(t) = \Pi_h - \mu_h N(t) - \delta_h I_h(t) \leq \Pi_h - \mu_h N(t). \tag{2}$$

Therefore,

$$\overline{\lim_{t\to\infty}} N_h(t) \leq \frac{\Pi_h}{\mu_h} = N_h^*. \tag{3}$$

where the notation $\overline{\lim_{t\to\infty}}$ (or $\limsup_{t\to\infty}$), represents the limit superior as t approaches infinity. If we presume the disease is not present in the population, Equation (2) reaches a single equilibrium point N_h^*, which is globally asymptotically stable (GAS). Furthermore, $N_h(t)$ remains bounded.

In a similar way, for the cattle subsystem outlined in (1), and assuming a positive initial condition, let

$$N_c(t) = S_c(t) + E_c(t) + I_c(t) + R_c(t).$$

Therefore, $N_c'(t) = \Pi_c - \mu_c N_c(t) - \delta_c I_c(t) \leq \Pi_c - \mu_c N_c(t)$ has a single equilibrium $N_c^* = \Pi_c/\mu_c$, which is globally asymptotically stable (GAS) and ensures that $N_c(t)$ remains bounded. Additionally, we have

$$\overline{\lim_{t\to\infty}} N_c(t) \leq \frac{\Pi_c}{\mu_c} = N_c^*. \tag{4}$$

We can derive from the last equation in (1) that $I_h \leq N_h \leq N_h^*$, $I_c \leq N_c \leq N_c^*$, and

$$\begin{aligned} B^{'}(t) &\leq \alpha_h N_h^* + \alpha_c N_c^* - \mu_b B(t), \\ F^{'}(t) &\leq \eta N_c^* - \mu_f F(t), \end{aligned} \tag{5}$$

which implies that F and B are non-negative and

$$\begin{aligned} \overline{\lim_{t\to\infty}} B(t) &\leq \frac{\alpha_h N_h^* + \alpha_c N_c^*}{\mu_b} = B^*, \\ \overline{\lim_{t\to\infty}} F(t) &\leq \frac{\eta N_c^*}{\mu_f} = F^*, \end{aligned} \tag{6}$$

and hence $B(t)$ and $F(t)$ remain bounded as well.

As a result, the previous analysis demonstrates that the solutions of system (1) are both bounded and non-negative within the specified region.

$$\Omega := \left\{ (S_h, I_h, R_h, S_c, E_c, I_c, B, F) \in \mathbb{R}_+^9 : \ N_h \leqslant N_h^*, \ N_c \leqslant N_c^*, \ B \leqslant B^*, \ F \leqslant F^* \right\}.$$

Consequently, we make the following proposition.

Proposition 1. *System (1) remains positively invariant within the region Ω. In particular, when the initial values are $\phi(0) \in \mathbb{R}_+^9$, then the solution $\big(S_h(t), I_h(t), R_h(t), S_c(t), E_c(t), I_c(t), B(t), F(t)\big)$ is positive for all $t > 0$.*

Proof. The non-negativity of the solutions of system (1) can be established by proving that if $\big(S_h(0), I_h(0), R_h(0), S_c(0), E_c(0), I_c(0), R_c(0), B(0), F(0)\big) \in \mathbb{R}_+^9$, the solutions of system (1), $\big(S_h(t), I_h(t), R_h(t), S_c(t), E_c(t), I_c(t), B(t), F(t)\big)$ remain non-negative for all $t > 0$. Consider the function

$$q_1(t) = \min\{S_h(t), I_h(t), R_h(t)\}, \ \forall t > 0.$$

Given $q_1(0) > 0$, one can hypothesize that a time $t_1 > 0$ where $q_1(t_1) = 0$ and $q_1(t) > 0$ is valid for all $t \in [0, t_1)$. Under the assumption of $q_1(t_1) = S_h(t_1)$, the first equation within System (1) leads to the subsequent inequality

$$S_h'(t) \geq -\big(\lambda_h(t) + \mu_h\big) S_h(t), \quad \forall t \in [0, t_1].$$

Consequently, $0 = S_h(t_1) \geq S_h(0) e^{-\int_0^{t_1} \left(\lambda_h(t) + \mu_h\right) ds} > 0$ follows. This contradiction arises due to the infeasibility of obtaining negative values for $S_h(t)$ for any $t > 0$.

We proceed by considering the existence of a minimum time value denoted as $t > 0$, at which point one of the compartments, specifically $I_h(t)$ or $R_h(t)$, becomes zero. Without loss of generality, assume that this compartment is $I_h(t)$. If $q_1(t_1) = I_h(t_1)$ holds, then employing the second equation of (1), we derive $B(t) \geq 0$, $F(t) \geq 0$, and $S_h(t) \geq 0$ for all $t \in [0, t_1]$. Consequently, we ascertain

$$I_h'(t) \geq -(\gamma_h + \delta_h + \mu_h) I_h(t), \quad \forall t \in [0, t_1].$$

This leads to

$$0 = I_h(t_1) \geq I_h(0)e^{-(\gamma_h+\delta_h+\mu_h)t_1} > 0,$$

resulting in a contradiction. Analogously, if $q_1(t_1) = R_h(t_1)$ were true, a similar contradiction would ensue. Hence, we deduce that $S_h(t) \geq 0$, $I_h(t) \geq 0$, and $R_h(t) \geq 0$ for every $t > 0$. Furthermore, equality is attained when the initial conditions are set to zero. Using Equation (2), we can represent $N_h(t)$ in terms of $N_h(0)e^{-\mu_h t} + \frac{\Pi_h}{\mu}(1 - e^{-\mu_h t})$, where $N_h(0) = S_h(0) + I_h(0) + R_h(0)$ is true. Consequently, $N(t)$ is bounded for all $t \geq 0$, leading to $\overline{\lim_{t\to\infty}} N_h(t) = \frac{\Pi_h}{\mu_h}$.

Consider $q_2(t) = \min\{S_c(t), E_c(t), I_c(t), R_c(t)\}$, $\forall t > 0$. Given $q_2(0) > 0$, we can posit the existence of a time point $t_2 > 0$ at which $q_2(t_2) = 0$ and that $q_2(t) > 0$ holds for all $t \in [0, t_2)$. By assuming $q_2(t_2) = S_c(t_2)$, System (1) results in the inequality

$$S_c'(t) \geq -\big(\lambda_c(t) + \mu_c\big)S_c(t), \quad \forall t \in [0, t_2].$$

Consequently, $0 = S_c(t_2) \geq S_c(0)e^{-\int_0^{t_2}\left(\lambda_c(t)+\mu_c\right)ds} > 0$. This contradiction emerges from the infeasibility of negative values for $S_c(t)$ for any $t > 0$. Likewise, an analogous conclusion can be deduced concerning $E_c(t)$, $I_c(t)$, and $R_c(t)$ by employing similar reasoning. According to (4), it is established that $N_c(t)$ remains bounded for any instance of $t \geq 0$, with the addition of $\overline{\lim_{t\to\infty}} N_c(t) = \frac{\Pi_c}{\mu_c}$. Furthermore, from (6), it can be deduced that $B(t)$ and $F(t)$ are bounded, leading to the inference that $S_h(t)$, $I_h(t)$, $R_h(t)$, $S_c(t)$, $E_c(t)$, $I_c(t)$, $R_c(t)$, $B(t)$, and $F(t)$ are consequently bounded for each instance of $t > 0$. Therefore, the proof is concluded. □

The system (1) reaches a disease-free equilibrium (DFE) when the disease is completely absent, as indicated by

$$\mathbf{E}^* = \big(S_h^*, I_h^*, R_h^*, S_c^*, E_c^*, I_c^*, B^*, F^*\big) = \big(\frac{\Pi_h}{\mu_h}, 0, 0, \frac{\Pi_c}{\mu_c}, 0, 0, 0, 0, 0\big), \tag{7}$$

and it is always feasible.

3. Basic Reproduction Number

In this section, we focus extensively on the calculation of $\mathcal{R}_0$, known as the basic reproduction number (BRN). This parameter is essential to characterize the periodic system described by Equation (1), as it provides information on the average number of secondary infections produced by an infected individual in a completely susceptible population over a specified period. We shall calculate the BRNP, denoted as $\mathcal{R}_0$, for Model (1) using the method suggested by Wang and Zhao [25].

The vector $\mathbf{X} = (I_h, E_c, I_c, B, F, S_h, R_h, S_c, R_c)^T$ describes the state of the system, with $\mathbf{F}(t, \mathbf{X}(t))$, $\mathbf{V}^+(t, \mathbf{X}(t))$, and $\mathbf{V}^-(t, \mathbf{X}(t))$ representing the rates of individuals newly infected, incoming from external sources, and exiting compartments, respectively. To satisfy conditions (A1)–(A7), as specified in ([25], Section 1), we have reformulated the system (1), which is presented as

$$\mathbf{X}'(t) = \mathbf{F}(t, \mathbf{X}(t)) - \mathbf{V}(t, \mathbf{X}(t)), \tag{8}$$

where $\mathbf{V}(t, \mathbf{X}(t)) = \mathbf{V}^-(t, \mathbf{X}(t)) - \mathbf{V}^+(t, \mathbf{X}(t))$.

In order to specify the DFE of (8), we consider $\mathbf{X}^* = \big(0, 0, 0, 0, 0, 0, S_h^*, 0, S_c^*, 0\big)$. To derive the matrices $\mathcal{F}(t)$ and $\mathcal{V}(t)$, we initially introduce $\mathcal{F}(t)$ as the matrix following $\big(\frac{\partial \mathbf{F}_i(t, \mathbf{X}^*)}{\partial \mathbf{X}_j}\big)_{1\leqslant i,j\leqslant 6}$ and the matrix $\mathcal{V}(t)$ is defined as $\big(\frac{\partial \mathbf{V}_i(t, \mathbf{X}^*)}{\partial \mathbf{X}_j}\big)_{1\leqslant i,j\leqslant 6}$. The entries of $\mathcal{F}(t)$ and $\mathcal{V}(t)$ are expressed as

$$\mathcal{F}(t) = \begin{bmatrix} \beta_h S_h^* & 0 & 0 & \beta_{bh}(t) S_h^* & \beta_f(t) S_h^* \\ 0 & 0 & 0 & 0 & 0 \\ 0 & 0 & \beta_c S_c^* & \beta_{bc}(t) S_c^* & 0 \\ 0 & 0 & 0 & 0 & 0 \\ 0 & 0 & 0 & 0 & 0 \end{bmatrix},$$

and

$$\mathcal{V}(t) = \begin{bmatrix} \gamma_h + \delta_h + \mu_h & 0 & 0 & 0 & 0 \\ 0 & \nu + \mu_c & 0 & 0 & 0 \\ 0 & -\nu & \gamma_c + \delta_c + \mu_c & 0 & 0 \\ -\alpha_h & 0 & -\alpha_c & \mu_b & 0 \\ 0 & 0 & -\eta & 0 & \mu_f \end{bmatrix}.$$

The verification of conditions (A1) to (A6), as outlined in [25], is straightforward, and the disease-free equilibrium $\mathbf{X}^*$ exhibits linear asymptotic stability at the point $\mathbf{X}_s = (0, 0, 0, 0, 0, S_h, R_h, S_c, R_c) \in \mathbb{R}_+^9$.

Let $\mathbf{Y}(y_1, y_2)$ be considered as a solution to the following initial value problem, assuming y_1 is greater than or equal to y_2:

$$\frac{\mathrm{d}\mathbf{Y}(y_1, y_2)}{\mathrm{d}t} = -\mathcal{V}(y_1)\mathbf{Y}(y_1, y_2), \qquad \mathbf{Y}(y_2, y_2) = I_6, \quad \forall y_1 \geqslant y_2. \tag{9}$$

The identity matrix I_6 represents a matrix 6×6. Consequently, condition (A7) in [25] is met because the matrix $\Phi_{-\mathcal{V}}(t)$ referred to in (9) for $t \geqslant 0$ is equivalent to $\mathbf{Y}(y, 0)$. Consider $\mathcal{C}_T$, the ordered Banach space composed of T-periodic functions that map $\mathbb{R}$ to $\mathbb{R}^6$, characterized by the $\|\cdot\|_\infty$ (usual maximum norm). We then define $\mathcal{C}_T^+ := \{\phi \in \mathcal{C}_T : \phi(t) \geqslant 0, \ \forall t \in \mathbb{R}\}$ as the positive cone.

The successive infection linear operator $\mathbf{K}$ is defined as the mapping of the space $\mathcal{C}_T$ onto itself. It can be expressed as

$$(\mathbf{K}\phi)(y) = \int_0^\infty \mathbf{Y}(y, y - r)\mathcal{F}(y - r)\phi(y - r)dr, \qquad \forall\, \phi \in \mathcal{C}_T, \ y \in \mathbb{R}.$$

The basic reproduction number $\mathcal{R}_0$ for the model (1) can be calculated by finding the spectral radius of $\mathbf{K}$; thus,

$$\mathcal{R}_0 := \rho(\mathbf{K}). \tag{10}$$

Consider $\Phi_{\mathcal{F}-\mathcal{V}}(t)$ as a fundamental matrix associated with the linear T-periodic system $\mathbf{y}' = [\mathcal{F}(t) - \mathcal{V}(t)]\mathbf{y}$. For simplicity, and without loss of generality, we assume $\Phi_{\mathcal{F}-\mathcal{V}}(0) = I$, which is the identity matrix. At this juncture, we note that $\Phi_{\mathcal{F}-\mathcal{V}}(T)$ serves as the monodromy matrix of this linear T-periodic system. In the analysis for the local stability of $\mathbf{E}^*$, as described in Equation (7), we refer to Theorem 2.2 from [25].

Theorem 1. *The relation between the BRNP and the monodromy matrix can be outlined as follows.*

1. $\mathcal{R}_0 = 1$ *is the same as* $\rho(\Phi_{\mathcal{F}-\mathcal{V}}(T)) = 1$;
2. $\mathcal{R}_0 > 1$ *is the same as* $\rho(\Phi_{\mathcal{F}-\mathcal{V}}(T)) > 1$;
3. $\mathcal{R}_0 < 1$ *is the same as* $\rho(\Phi_{\mathcal{F}-\mathcal{V}}(T)) < 1$.

The inequalities presented in Theorem 1 correspond to the stability of the origin in the periodic system $x' = [\mathcal{F}(t) - \mathcal{V}(t)]x$, as characterized by the traditional Floquet theory.

4. Threshold Dynamics

This section seeks to demonstrate that $\mathbf{E}^*$, as defined in (7), exhibits global asymptotic stability (GAS) and that Salmonella is eradicated when the basic reproduction number $\mathcal{R}_0$, defined in (10), is below 1. When $\mathcal{R}_0 < 1$, the disease-free equilibrium $\mathbf{E}^*$ is globally asymptotically stable, indicating that Salmonella will eventually die out as each infected individual generates fewer than one new infection. In contrast, if $\mathcal{R}_0 > 1$, the disease persists, and we establish the existence of a positive periodic solution in (1), reflecting the sustained presence of Salmonella in the population. This highlights the critical role of $\mathcal{R}_0$ as a threshold for Salmonella control, emphasizing the need for interventions to reduce transmission and prevent outbreaks. To confirm the GAS of the disease-free equilibrium (DFE) $\mathbf{E}^*$ and the persistence of the disease, the following lemma will be used.

Lemma 1 ([26], Lemma 2.1)**.** *Let* $\zeta = \frac{1}{T}\ln\rho(\Phi_{D(\cdot)}(T))$. *Under this assumption, there is a positive T-periodic function* $u(t)$ *such that* $e^{\zeta t}u(t)$ *represents a solution to the equation* $z' = D(t)z$.

4.1. Local Stability of the DFE $\mathbf{E}^*$

Based on the findings discussed in Section 3, we present the following Theorem concerning the local asymptotic stability (LAS) of $\mathbf{E}^*$, as defined in (7) within the framework of model (1).

Theorem 2. *When* $\mathcal{R}_0 < 1$, *the disease-free equilibrium (DFE)* $\mathbf{E}^*$, *as characterized in* (7), *exhibits local asymptotic stability. In contrast, if* $\mathcal{R}_0 > 1$, $\mathbf{E}^*$ *becomes unstable.*

Proof. The Jacobian matrix $\mathcal{J}(t)$ of the system characterized by Equation (1) at the equilibrium point $\mathbf{E}^*$ is given by

$$\mathcal{J}(t) = \begin{bmatrix} \mathcal{F}(t) - \mathcal{V}(t) & 0 \\ -\mathcal{A}(t) & M \end{bmatrix},$$

where M and $\mathcal{A}(t)$ are defined by

$$\mathcal{A}(t) = \begin{bmatrix} \beta_h S_h^* & 0 & 0 & \beta_{bh}(t)S_h^* & \beta_f(t)S_h^* \\ \gamma_h & 0 & 0 & 0 & 0 \\ 0 & 0 & \beta_c S_c^* & \beta_{bc}(t)S_c^* & 0 \\ 0 & 0 & \gamma_h & 0 & 0 \end{bmatrix},$$

and

$$M = \begin{bmatrix} -\mu_h & \omega_h & 0 & 0 \\ 0 & -\omega_h - \mu_h & 0 & 0 \\ 0 & 0 & -\mu_c & \omega_c \\ 0 & 0 & 0 & -\omega_c - \mu_c \end{bmatrix}.$$

The matrix M, characterized by eigenvalues $-\mu_h$, $-\omega_h - \mu_h$, $-\mu_c$, and $-\omega_c - \mu_c$, is constant. Since all these eigenvalues are negative, it follows that $\rho(\Phi_M) < 1$. As reported in [27], the linear asymptotic stability (LAS) of $\mathbf{E}^*$ is dictated by conditions $\rho(\Phi_{\mathcal{F}-\mathcal{V}}(T)) < 1$ and $\rho(\Phi_M(T)) < 1$. Consequently, the stability of the DFE $\mathbf{E}^*$ is entirely dependent on the magnitude of $\rho(\Phi_{\mathcal{F}-\mathcal{V}}(T))$. Therefore, the equilibrium point $\mathbf{E}^*$ is deemed unstable when $\rho(\Phi_{\mathcal{F}-\mathcal{V}}(T)) > 1$, and it achieves local asymptotic stability (LAS) when $\rho(\Phi_{\mathcal{F}-\mathcal{V}}(T)) < 1$. The proof concludes with the result presented in Theorem 1. □

4.2. Global Stability of the DFE $\mathbf{E}^*$

Theorem 3. *When* $\mathcal{R}_0 < 1$, *the disease-free equilibrium, denoted as* $\mathbf{E}^*$, *is globally asymptotically stable.*

Proof. According to the local stability analysis presented in Theorem 2, $\mathbf{E}^*$ is LAS when $\mathcal{R}_0 < 1$. However, it remains essential to establish that $\mathbf{E}^*$ is globally attractive. As discussed in Section 3, criteria (A1) to (A7), as outlined in [28], are satisfied. Moreover, $\mathbf{X}^* = (0, 0, 0, 0, 0, 0, S_h^*, 0, S_c^*, 0)$ denotes the unique periodic solution of (8) within the domain of disease-free equilibria $\mathbf{X}_s$. When considering the initial equations of (1), the resulting expression is:

$$S_h^{'}(t) = \Pi_h - \lambda_h(t)S_h(t) - \mu_h S_h(t) + \omega_h R_h(t),$$
$$S_c^{'}(t) = \Pi_c - \lambda_c(t)S_c(t) - \mu_c S_c(t) + \omega_c R_c(t).$$

Because $I_h(t) \geq 0$, $I_c(t) \geq 0$, $B(t) \geq 0$, and $F(t) \geq 0$, One can prove that $S_h^{'}(t) \leq \Pi_h - \mu_h S_h(t)$ and $S_c^{'}(t) \leq \Pi_c - \mu_c S_c(t)$, meaning that

$$\overline{\lim_{t\to\infty}} S_h(t) \leq \frac{\Pi_h}{\mu_h} = S_h^* \quad \text{and} \quad \overline{\lim_{t\to\infty}} S_c(t) \leq \frac{\Pi_c}{\mu_c} = S_c^*.$$

Therefore, there exists a time $t(\varepsilon) > 0$ such that for any given $\varepsilon > 0$, the inequality $S_h(t) \leq S_h^* + \varepsilon$ and $S_c(t) \leq S_c^* + \varepsilon$ holds for all $t > t(\varepsilon)$. By referring to (1), for $t > t(\varepsilon)$, we observe that

$$\begin{aligned}
I_h^{'}(t) &\leq \lambda_h(t)(S_h^* + \varepsilon) - (\gamma_h + \delta_h + \mu_h)I_h(t),\\
E_c^{'}(t) &\leq \lambda_c(t)(S_c^* + \varepsilon) - (\nu + \mu_c)E_c(t),\\
I_c^{'}(t) &\leq \nu E_c(t) - (\gamma_c + \delta_c + \mu_c)I_c(t),\\
B^{'}(t) &\leq \alpha_h I_h(t) + \alpha_c I_c(t) - \mu_b B(t),\\
F^{'}(t) &\leq \eta I_c(t) - \mu_f F(t),
\end{aligned}$$

We define $\mu(\varepsilon) := \min\{S_h^*/(S_h^* + \varepsilon), S_c^*/(S_c^* + \varepsilon)\}$, which leads us to the system:

$$G'(t) \leqslant \left(\frac{\mathcal{F}(t)}{\mu(\varepsilon)} - \mathcal{V}(t)\right)G(t), \quad \forall t \geqslant t(\varepsilon), \tag{11}$$

with $G(t) = (I_h(t), E_c(t), I_c(t), B(t), F(t))$. As t tends to infinity, $G(t)$ converges to zero, resulting in disease eradication. By applying Theorem 2 [28], we infer that $\mathbf{X}^*$ possesses global asymptotic stability (GAS) due to its GAS properties within the disease-free subspace $\mathbf{X}_s$. □

4.3. Existence of Endemic Periodic Solutions

Our subsequent step involves presenting the symbols and notations that will be utilized:

$$X := \left\{(S_h, I_h, R_h, S_c, I_c, E_c, R_c, B, F) \in \mathbb{R}_+^9\right\},$$
$$X_0 := \left\{(S_h, I_h, R_h, S_c, I_c, E_c, R_c, B, F) \in X\colon\ I_h > 0, E_c > 0, I_c > 0, B > 0, F > 0\right\},$$

and

$$\partial X_0 := X \setminus X_0 = \{(S_h, I_h, R_h, S_c, I_c, E_c, R_c, B, F) \in X :\ I_h E_c I_c B F = 0\}.$$

The Poincaré map, denoted as $\mathcal{P}\colon \mathbb{R}_+^9 \to \mathbb{R}_+^9$, is defined in relation to (1). Specifically, $\mathcal{P}(x^0)$ is given by the function $u(T, x^0)$, where $x^0 \in \mathbb{R}_+^9$. Here, $u(t, x^0)$ refers to the unique solution of (1) with the initial condition specified by x^0. It follows that, for all $m \geqslant 0$, we have $\mathcal{P}^m(x^0) = u(mT, x^0)$.

Lemma 2. *Given any $\psi(0) \in X_0$ such that $\|\psi(0) - \mathbf{E}^*\| \leqslant \sigma$ for $\sigma > 0$, if $\mathcal{R}_0 > 1$, then the subsequent inequality is satisfied:*

$$\overline{\lim_{m\to\infty}} \mathrm{d}(\mathcal{P}^m(\psi(0)), \mathbf{E}^*) \geqslant \sigma.$$

Proof. Utilizing Theorem 1, it follows that $\rho(\Phi_{\mathcal{F}-\mathcal{V}}(T))$ exceeds 1 whenever $\mathcal{R}_0$ is more than 1. Consequently, there exists a sufficiently small $\varrho > 0$ such that $\rho(\Phi_{\mathcal{F}-\mathcal{V}-M_\varrho}(T)) > 1$, where

$$M_\varrho(t) = \begin{bmatrix} \beta_h\varrho & 0 & 0 & \beta_{bh}(t)\varrho & \beta_f(t)\varrho \\ 0 & 0 & 0 & 0 & 0 \\ 0 & 0 & \beta_c\varrho & \beta_{bc}(t)\varrho & 0 \\ 0 & 0 & 0 & 0 & 0 \\ 0 & 0 & 0 & 0 & 0 \end{bmatrix}.$$

Consider an arbitrary constant $\varrho > 0$. There is a corresponding positive constant $\sigma = \sigma(\varrho)$ such that for any $\psi(0) \in X_0$ that satisfies $\|\psi(0) - \mathbf{E}^*\| \leqslant \sigma$, the continuous dependence of solutions on the initial conditions guarantees the validity of the following inequality:

$$\|u(t, \psi(0)) - u(t, \mathbf{E}^*)\| \leqslant \varrho, \ \ 0 \leqslant t \leqslant T.$$

Our next claim is that

$$\overline{\lim_{m\to\infty}} \mathrm{d}(\mathcal{P}^m(\psi(0)), \mathbf{E}^*) \geqslant \sigma. \tag{12}$$

Suppose that (12) does not hold, we then obtain

$$\overline{\lim_{m\to\infty}} \mathrm{d}(\mathcal{P}^m(\psi(0)), \mathbf{E}^*) < \sigma, \tag{13}$$

holds for some $\psi(0) \in X_0$. It is possible to adopt a simplified assumption that

$$\mathrm{d}(\mathcal{P}^m(\psi(0)), \mathbf{E}^*) < \sigma, \quad \forall m \geq 0.$$

The aforementioned details suggest

$$\|u(t, \mathcal{P}^m(\psi(0)) - u(t, \mathbf{E}^*)\| < \varrho, \ \forall 0 \leqslant t \leqslant T, \ m \geq 0.$$

Let $t \geqslant 0$ be represented by $t = t_1 + mT$, where $0 \leqslant t_1 < T$ and $m = \lfloor \frac{t}{T} \rfloor$, representing the greatest integer less than or equal to $\frac{t}{T}$. By using this formulation, we derive

$$\|u(t, \psi(0)) - u(t, \mathbf{E}^*)\| = \|u(t_1, \mathcal{P}^m(\psi(0)) - u(t_1, \mathbf{E}^*)\| < \varrho,$$

for all $t \geqslant 0$, suggesting that $S_h(t) \geqslant S_h^* - \varrho$ and $S_c(t) \geqslant S_c^* - \varrho$. Then, for

$$\|\psi(0) - \mathbf{E}^*\| \leqslant \sigma,$$

we derive

$$\begin{aligned}
I_h^{'}(t) &\geq \lambda_h(t)(S_h^* - \varrho) - \gamma_h I_h(t) - (\delta_h + \mu_h) I_h(t), \\
E_c^{'}(t) &\geq \lambda_c(t)(S_c^* - \varrho) - \nu E_c(t) - \mu_c E_c(t), \\
I_c^{'}(t) &\geq \nu E_c(t) - \gamma_c I_c(t) - (\delta_c + \mu_c) I_c(t), \\
B^{'}(t) &\geq \alpha_h I_h(t) + \alpha_c I_c(t) - \mu_b B(t), \\
F^{'}(t) &\geq \eta I_c(t) - \mu_f F(t).
\end{aligned}$$

The system presented below is utilized as an auxiliary system,

$$\begin{aligned} I_h^{'}(t) &= \lambda_h(t)(S_h^* - \varrho) - \gamma_h I_h(t) - (\delta_h + \mu_h) I_h(t), \\ E_c^{'}(t) &= \lambda_c(t)(S_c^* - \varrho) - \nu E_c(t) - \mu_c E_c(t), \\ I_c^{'}(t) &= \nu E_c(t) - \gamma_c I_c(t) - (\delta_c + \mu_c) I_c(t), \\ B^{'}(t) &= \alpha_h I_h(t) + \alpha_c I_c(t) - \mu_b B(t), \\ F^{'}(t) &= \eta I_c(t) - \mu_f F(t). \end{aligned} \tag{14}$$

From our preceding discourse, we can deduce that $\rho(\Phi_{\mathcal{F}-\mathcal{V}-M_\varrho}(T)) > 1$. According to Lemma 1, there is a function $p(t) > 0$ that is periodic with period T and serves as a solution to (14) in the form $p(t)\exp(\zeta t)$, where $\zeta = \frac{1}{T}\ln\rho(\Phi_{\mathcal{F}-\mathcal{V}-M_\varrho}(T)) > 0$. For every initial condition $H(0) \in \mathbb{R}^6_+$, there exists a constant $K^* \in \mathbb{R}_+$ such that the inequality $H(0) \geqslant K^* p(0)$ is satisfied. Here, $H(t)$ is defined as $H(t) = (I_h(t), E_c(t), I_c(t), B(t), F(t))^T$, and in accordance with Theorem B.1 from [29], the inequality $H(t) \geqslant p(t)\exp(\zeta t)$ holds for all $t > 0$. As a result, we can infer that $\lim_{t\to\infty} I_h(t) = \infty$, $\lim_{t\to\infty} E_c(t) = \infty$, $\lim_{t\to\infty} I_c(t) = \infty$, $\lim_{t\to\infty} B(t) = \infty$, and $\lim_{t\to\infty} F(t) = \infty$, leading to a contradiction to $I_h(t) < \varrho$, $E_c(t) < \varrho$, $I_c(t) < \varrho$, $B(t) < \varrho$, $F(t) < \varrho$, and Equation (13). Thus, the proof is complete, as we have verified the correctness of Equation (12). □

Theorem 4. *Assume $\mathcal{R}_0 > 1$. Under these conditions, system (1) possesses at least one positive periodic solution.*

Proof. Our objective is to demonstrate the uniform persistence of $\mathcal{P}$ concerning $(X_0, \partial X_0)$. This demonstration will indicate that the solution to equation (1) is likewise uniformly persistent regarding $(X_0, \partial X_0)$, as supported by ([30], Theorem 3.1.1). Initially, it is essential to establish that both ∂X_0 and X_0 are positively invariant under the dynamics of system (1).

Assuming $\big(S_h(0), I_h(0), R_h(0), S_c(0), E_c(0), I_c(0), R_c(0), B(0), F(0)\big) \in X_0$, one can resolve (1) for any $t > 0$ in order to derive

$$S_1(t) = \Big[S_h(0) + \int_0^t (\Pi_h + \omega_h R_h(s)) e^{\int_0^s (\lambda_h(r)+\mu_h)\,dr}\,ds\Big] e^{\int_0^t -(\lambda_h(r)+\mu_h)\,dr} > 0, \tag{15}$$

$$I_h(t) = \Big[I_h(0) + \int_0^t \lambda_h(S) S_h(s) e^{(\gamma_h+\delta_h+\mu_h)s}\,ds\Big] e^{-(\gamma_h+\delta_h+\mu_h)t} > 0, \tag{16}$$

$$R_h(t) = \Big[R_h(0) + \int_0^t \gamma_h I_h(s) e^{(\omega_h+\mu_h)s}\,ds\Big] e^{-(\omega_h+\mu_h)t} > 0, \tag{17}$$

$$S_c(t) = \Big[S_c(0) + \int_0^t (\Pi_c + \omega_c R_c(s)) e^{\int_0^s (\lambda_c(r)+\mu_c)\,dr}\,ds\Big] e^{\int_0^t -(\lambda_c(r)+\mu_c)\,dr} > 0, \tag{18}$$

$$E_c(t) = \Big[E_c(0) + \int_0^t \lambda_c(s) S_c(s) e^{(\nu+\mu_c)s}\,ds\Big] e^{-(\nu+\mu_c)t} > 0, \tag{19}$$

$$I_c(t) = \Big[I_c(0) + \nu \int_0^t E_c(s) e^{(\gamma_c+\delta_c+\mu_c)s}\,ds\Big] e^{-(\gamma_c+\delta_c+\mu_c)t} > 0, \tag{20}$$

$$R_c(t) = \Big[R_c(0) + \int_0^t \gamma_c I_c(s) e^{(\omega_c+\mu_c)s}\,ds\Big] e^{-(\omega_c+\mu_c)t} > 0, \tag{21}$$

$$B(t) = \Big[B(0) + \int_0^t (\alpha_h I_h(s) + \alpha_c I_c(s)) e^{\mu_b s}\,ds\Big] e^{-\mu_b t} > 0, \tag{22}$$

$$F(t) = \Big[F(0) + \int_0^t \gamma\eta I_c(s) e^{\mu_f s}\,ds\Big] e^{-\mu_f t} > 0, \tag{23}$$

Consequently, we have demonstrated that X_0 maintains positive invariance with respect to the dynamics governed by Equation (1). Furthermore, given that ∂X_0 is relatively closed

within X, we can infer that ∂X_0 also retains positive invariance, and therefore, System (1) exhibits point dissipative characteristics. Defining

$$M_\partial = \{(S_h(0), I_h(0), R_h(0), S_c(0), E_c(0), I_c(0), R_c(0), B(0), F(0)) \in \partial X_0 : P^m(S_h(0), I_h(0), R_h(0), S_c(0), E_c(0), I_c(0), R_c(0), B(0), F(0)) \in \partial X_0, \ \forall m \geqslant 0\}.$$

Our result will be demonstrated using the uniform persistence framework described in [30]. Specifically, it is crucial to show that the relationship $M_\partial = \mathcal{M}_\partial$ holds, with $\mathcal{M}_\partial$ defined as

$$\mathcal{M}_\partial = \{(S_h(0), I_h(0), R_h(0), S_c(0), E_c(0), I_c(0), R_c(0), B(0), F(0)) \in \partial X_0 : I_h(0) = R_h(0) = E_c(0) = I_c(0) = R_c(0) = B(0) = F(0) = 0\}.$$

It is evident that M_∂ includes $\mathcal{M}_\partial$. To finish the proof, it is necessary to show that M_∂ is a subset of $\mathcal{M}_\partial$. In other words, for any $(S_h(0), I_h(0), R_h(0), S_c(0), E_c(0), I_c(0), R_c(0), B(0), F(0)) \in \partial X_0$, at least one of the following conditions is satisfied: $I_h(nT) = 0$, $R_h(nT) = 0$, $E_c(nT) = 0$, $I_c(nT) = 0$, $R_c(nT) = 0$, $B(nT) = 0$, or $F(nT) = 0$, for any $n \geqslant 0$.

Suppose by contradiction that there exists a non-negative integer n_1 for which $I_h(nT)$, $R_h(nT)$, $E_c(nT)$, $I_c(nT)$, $R_c(nT)$, $B(nT)$, $F(nT)$ are all positive. By introducing the substitution $t = n_1 T$ into Equations (15) to (23), we obtain the result that $0 < S_h(t)$, $0 < I_h(t)$, $0 < R_h(t)$, $0 < S_c(t)$, $0 < E_c(t)$, $0 < I_c(t)$, $0 < R_c(t)$, $0 < B(t)$, $0 < F(t)$. This assertion contradicts the well-established fact that ∂X_0 is positively invariant.

According to Lemma 2, given the scenario where $\mathcal{R}_0 > 1$, we have demonstrated the weak uniform persistence of $\mathcal{P}$ relative to $(X_0, \partial X_0)$. Therefore, according to Proposition 1, it follows that $\mathcal{P}$ possesses a global attractor, while the set $\mathbf{E}^*$ emerges as an isolated invariant subset within X, such that the intersection of $W^s(\mathbf{E}^*)$ with X_0 is void: $W^s(\mathbf{E}^*) \cap X_0 = \emptyset$. Moreover, each solution within M_∂ converges to $\mathbf{E}^*$, and $\mathbf{E}^*$ exhibits acyclic behavior in M_∂. According to Theorem 1.3.1, Remark 1.3.1 in [30], it follows that $\mathcal{P}$ maintains uniform persistence relative to the pair $(X_0, \partial X_0)$. Therefore, there exists $\varepsilon > 0$ such that

$$\liminf_{t\to\infty} I_h(t) \geqslant \varepsilon, \quad \liminf_{t\to\infty} R_h(t) \geqslant \varepsilon, \quad \liminf_{t\to\infty} E_c(t) \geqslant \varepsilon, \quad \liminf_{t\to\infty} I_c(t) \geqslant \varepsilon,$$
$$\liminf_{t\to\infty} R_c(t) \geqslant \varepsilon, \quad \liminf_{t\to\infty} B(t) \geqslant \varepsilon, \quad \liminf_{t\to\infty} F(t) \geqslant \varepsilon.$$

In line with Theorem 1.3.6 from ([30]), an element $\tilde{\phi} \in X_0$ serves as an equilibrium point for $\mathcal{P}$, thereby indicating the presence of at least one periodic solution $u(t, \tilde{\phi})$ corresponding to (1). Here, $\tilde{\phi}$ is given by $(\tilde{S}_h(0), \tilde{I}_h(0), \tilde{R}_h(0), \tilde{S}_c(0), \tilde{E}_c(0), \tilde{I}_c(0), \tilde{R}_c(0), \tilde{B}(0), \tilde{F}(0)) \in X_0$. To show that $\tilde{S}_h(0)$ and $\tilde{S}_c(0)$ are positive, suppose otherwise, i.e., $\tilde{S}_h(0) = \tilde{S}_c(0) = 0$. Given the periodic nature of u for each $n \geqslant 0$, it follows that $\tilde{S}_h(nT) = \tilde{S}_c(nT) = 0$. This situation, however, results in a contradiction because it breaches the condition of positive invariance within X_0. Therefore, it must be that $\tilde{S}_h(0) > 0$ and $\tilde{S}_c(0) > 0$ for every $t > 0$. □

5. Numerical Simulations

In this section, we focus on presenting comprehensive numerical simulations that serve a dual purpose: to illustrate and substantiate the theoretical results elaborated upon in earlier sections. These simulations offer significant visual proofs of the concordance between our periodic model as defined in Equation (1) and the empirical observations of seasonal fluctuations. This alignment distinctly demonstrates the practical applicability of our theoretical framework in accounting for the observed periodic phenomena.

Salmonella infections show a notable seasonal variation, with a maximum transmission risk during the warmer months of the year. This pattern is primarily driven by

environmental factors, such as temperature, which facilitates bacterial growth, and human behavioral factors, such as increased outdoor food preparation. These dynamics make summer a high-risk period for Salmonella transmission.

In this work, we model the seasonal transmission of Salmonella using a sinusoidal function, peaking in August, to align with epidemiological observations for temperate regions. The seasonal variation is modeled using a sinusoidal function of the form:

$$f(t) = A \sin\left(2\pi \frac{t-\phi}{P}\right) + C,$$

where A is the amplitude, representing the intensity of the seasonal variation, P is the period to capture the yearly cycle, ϕ is the phase change that determines the peak time, and C is the vertical shift, representing the baseline level of transmission risk. For modeling Salmonella transmission, the parameters are chosen as follows: $A = 1$ to normalize the intensity of seasonal variation, $P = 365$ to reflect the annual periodicity of the transmission pattern, $C = 1$ to establish a baseline level of risk, and ϕ to align the peak transmission risk with August (Month 8), consistent with observed epidemiological trends.

We assume that $\beta_{bh}(t) = \bar{\beta}_{bh}\left(\sin\left(2\pi\frac{t-\phi}{P}\right)+1\right)$, $\beta_{bc}(t) = \bar{\beta}_{bc}\left(\sin\left(2\pi\frac{t-\phi}{P}\right)+1\right)$ and $\beta_f(t) = \bar{\beta}_f\left(\sin\left(2\pi\frac{t-\phi}{P}\right)+1\right)$ where $\bar{\beta}_{bh}$, $\bar{\beta}_{bh}$, and $\bar{\beta}_f$ are the baseline long-period transmission rate.

5.1. Model Collaboration to Salmonella Data from Saudi Arabia

To investigate the documented Salmonella outbreak in Saudi Arabia from 2018 to 2021, we analyzed time series data on cumulative annual cases and newly infected cases per year obtained from [31]. Parameter estimation for Model (1) was carried out using a combination of Latin hypercube sampling and least squares techniques [32], which allowed us to effectively calibrate the model. By fitting the data to Model (1), we derived parameter values that accurately describe the dynamics of the outbreak. The World Bank report on Saudi Arabia [33] in 2021 indicates a total population of 36,408,820 with a life expectancy at birth of 78 years. This results in a daily birth rate of approximately $\Pi_h = \mu_h \times N_h = 1297.75$, where μ_h is determined as $1/(365 \times 78)$.

The performance of the model in fitting the Salmonella data from Saudi Arabia is depicted in Figure 2. The left panel shows the comparison between the model and the cumulative cases of infection observed, while the right panel highlights the fit for newly infected cases. Both panels demonstrate that the model successfully replicates the observed trends of Salmonella during the 2018–2021 outbreak. Table 2 provides a detailed summary of the parameter values, their ranges, and associated units that resulted in the optimal fit. Using these parameters and the approach described in Mitchell and Kribs [34], the basic reproduction number, $\mathcal{R}_0$, was calculated to be approximately 0.606602. With $\mathcal{R}_0$ below the threshold of 1, the results suggest that disease transmission cannot be sustained indefinitely and is likely to die out in the population over time. Figure 3 indicates that the number of newly infected cases is projected to gradually decrease, approaching zero within a few years. Consequently, the cumulative number of Salmonella cases is expected to stabilize at approximately 40,000, reaching a steady state that remains constant over time.

Table 2. Parameter values, ranges, and units for Model (1).

Parameters	Fit and Extinction	Units	Range	Source	Persistence
Π_h	1278.85	humans	–	[33]	1278.85
μ_h	3.5×10^{-7}	day^{-1}	–	[33]	2×10^{-7}
β_{bc}	10^{-9}	$\text{cell}^{-1}\ \text{day}^{-1}$	10^{-15}–10^{-5}	Fitted	1.88×10^{-7}
β_{bh}	10^{-9}	$\text{cell}^{-1}\ \text{day}^{-1}$	10^{-15}–10^{-5}	Fitted	10^{-10}
β_c	10^{-9}	$\text{cattle}^{-1}\ \text{day}^{-1}$	10^{-15}–10^{-5}	Fitted	1.22×10^{-7}
β_f	10^{-9}	$\text{cell}^{-1}\ \text{day}^{-1}$	10^{-15}–10^{-5}	Fitted	6×10^{-9}
β_h	5×10^{-9}	$\text{humans}^{-1}\ \text{day}^{-1}$	10^{-15}–10^{-5}	Fitted	10^{-10}
α_c	0.0025	$\text{cells cattle}^{-1}\ \text{day}^{-1}$	10^{-5}–0.1	Fitted	0.0764
α_h	0.0025	$\text{cells humans}^{-1}\ \text{day}^{-1}$	10^{-5}–0.1	Fitted	0.0324
γ_c	0.1	day^{-1}	0–0.75	Fitted	0.009
γ_h	0.15	day^{-1}	0–0.75	Fitted	0.106
δ_c	0.143	day^{-1}	0–0.3	Fitted	0.255
δ_h	0.143	day^{-1}	0–0.3	Fitted	0.361
η	0.083	$\text{cells cattle}^{-1}\ \text{day}^{-1}$	10^{-3}–0.1	Fitted	0.083
μ_b	0.119	day^{-1}	–	Assumed	0.0275
μ_c	0.03	day^{-1}	–	Assumed	0.0275
μ_f	0.13	day^{-1}	–	Assumed	0.142
ν	0.102	day^{-1}	10^{-3}–0.75	Fitted	0.412
Π_c	500	cattle	–	Assumed	15600
ω_c	0.01	day^{-1}	10^{-3}–0.1	Fitted	0.00865
ω_h	0.0814	day^{-1}	10^{-3}–0.1	Fitted	0.0634

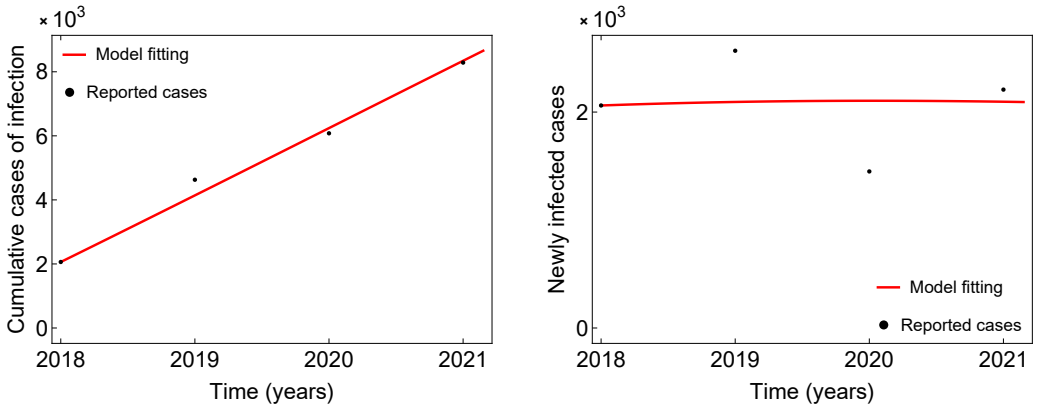

Figure 2. Fitting results of the model to data from Saudi Arabia (2018–2021), showing cumulative infected cases (**left**) and newly infected cases (**right**). The parameter values used for the fitting are provided in Table 2.

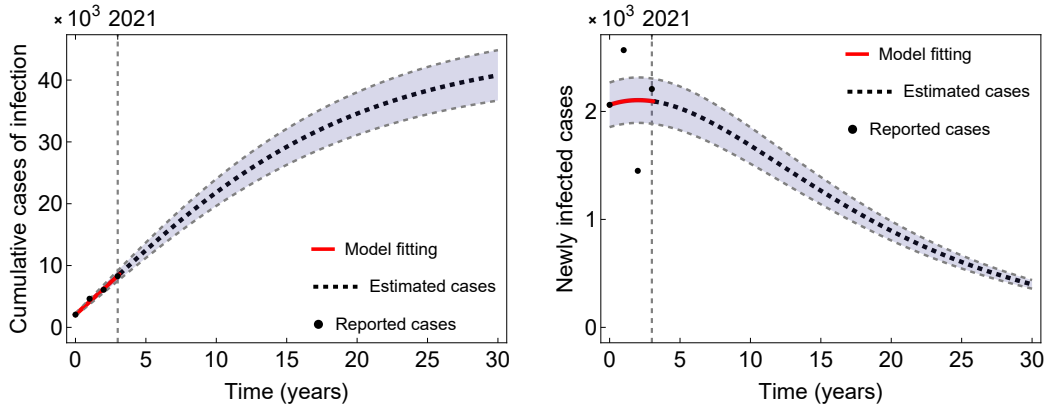

Figure 3. The predicted trajectory of new Salmonella infections in Saudi Arabia is illustrated using the parameter values detailed in Table 2.

5.2. Extinction of the Disease and the Existence of Periodic Solutions

To validate the theoretical findings, we performed numerical simulations that align with the time-periodic model, providing visual evidence of its consistency with observed seasonal fluctuations.

As discussed in Section 4, the basic reproduction number ($\mathcal{R}_0$) is a critical threshold parameter that determines whether the disease will persist or eventually die out in the population. The results presented in Figure 4 confirm the analytical predictions. Specifically, when $\mathcal{R}_0 \approx 0.606602 < 1$, the disease-free equilibrium $\mathbf{E}^*$ exhibits global asymptotic stability, which ultimately leads to the extinction of the disease in the population.

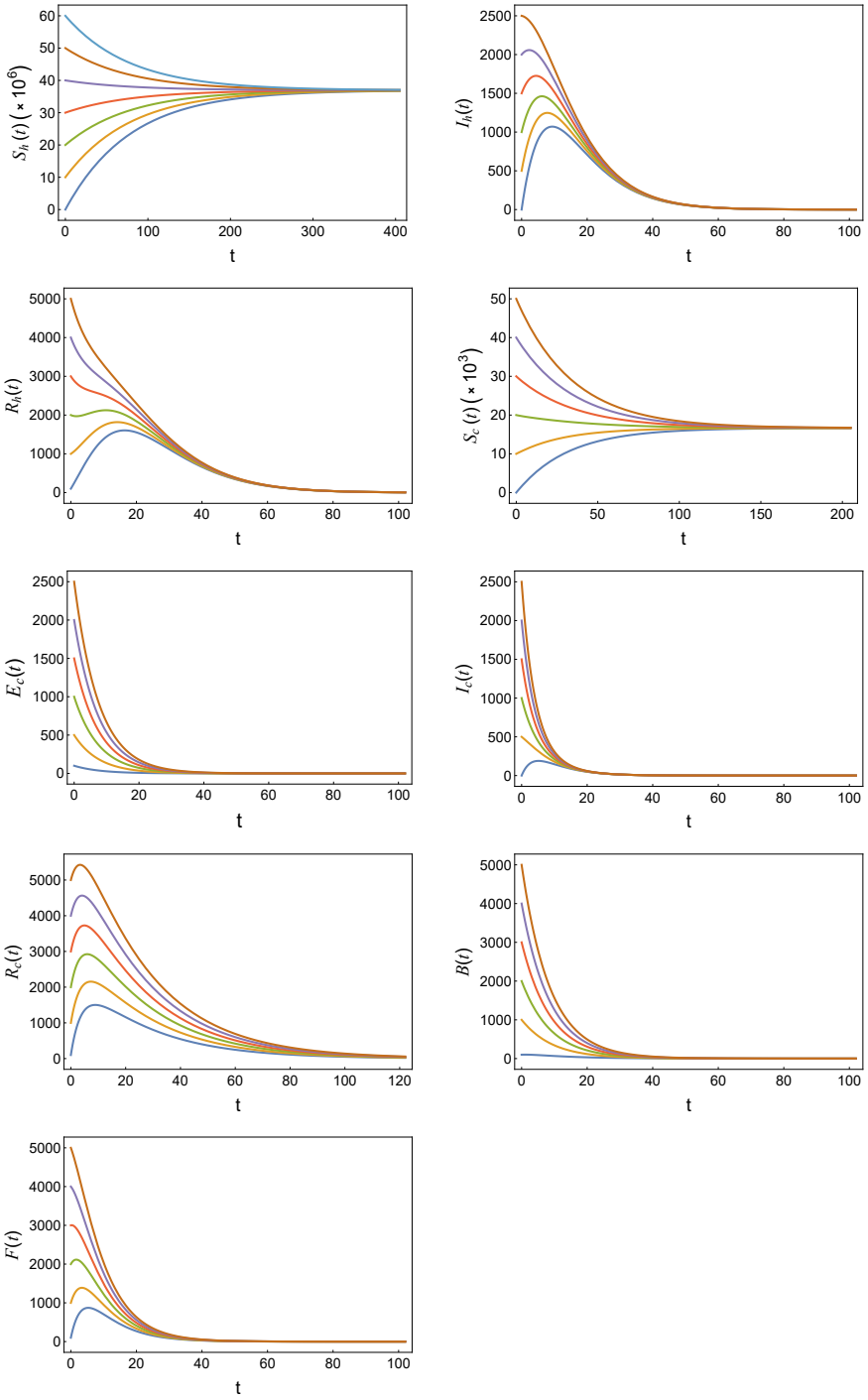

Figure 4. Extinction of Salmonella when $\mathcal{R}_0 = 0.6066 < 1$, given the specific parameter values specified in Table 2 (extinction).

Figures 5–7 illustrate the persistent dynamics of the disease when $\mathcal{R}_0 \approx 6.97762 > 1$, indicating the formation of an endemic state within the population. The high value $\mathcal{R}_0$ reflects persistent disease transmission, characterized by recurring annual outbreaks and the long-term stability of infection compartments. Simulations carried out using the parameter set of Table 2 further emphasize this persistence. These results demonstrate a direct link between elevated $\mathcal{R}_0$ and the continued presence of infections, confirming the existence of a stable positive periodic solution, as shown in Figures 6 and 7.

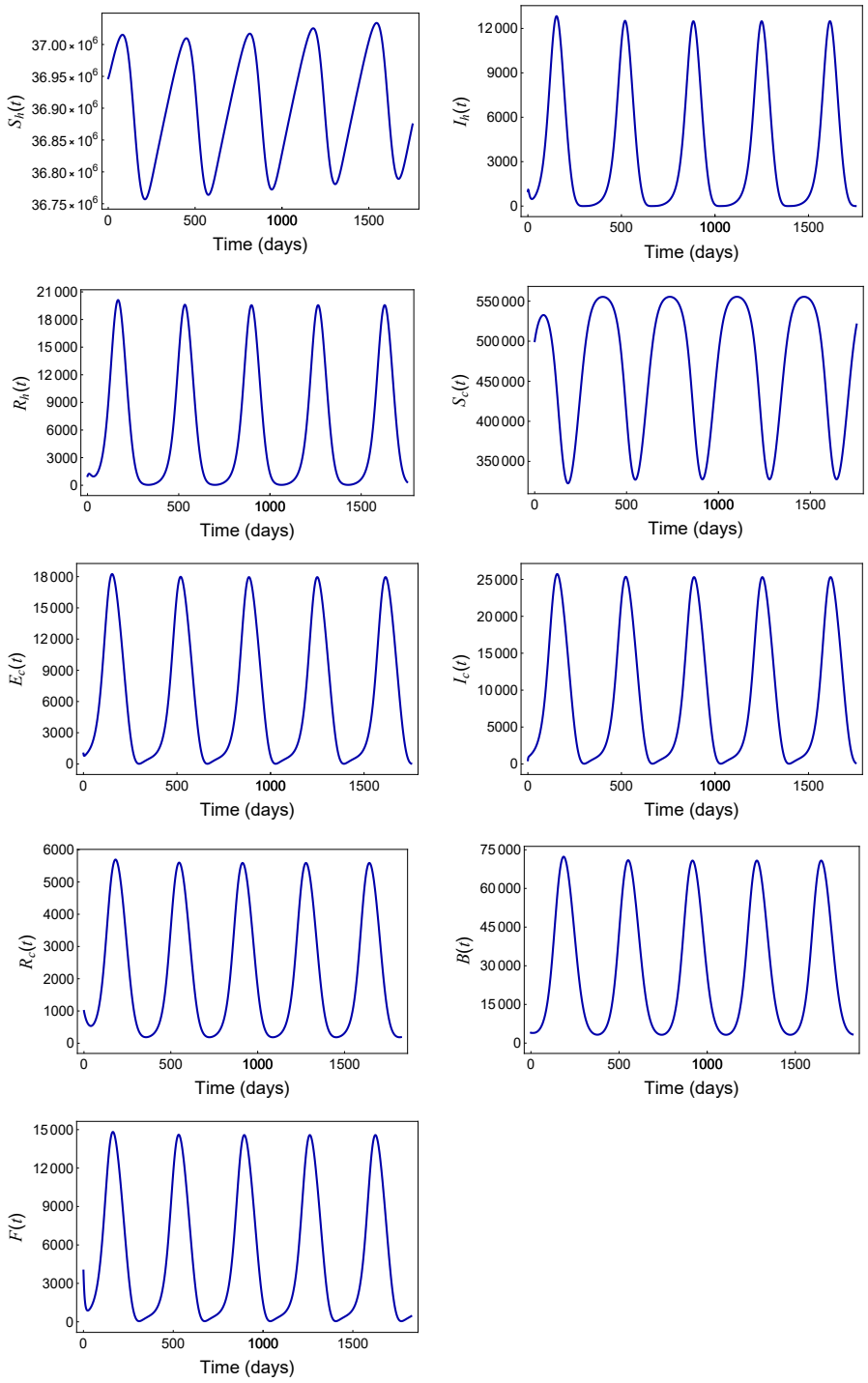

Figure 5. Persistence of Salmonella when $\mathcal{R}_0 = 6.97762 > 1$, given the specific parameter values specified in Table 2 (persistence).

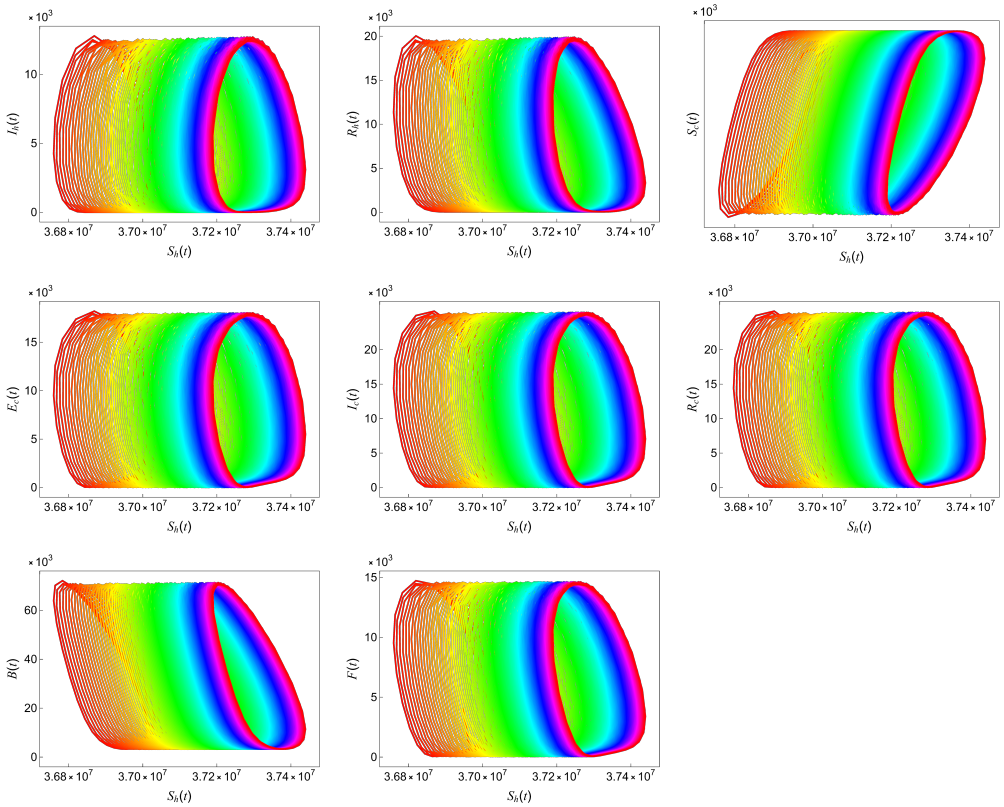

Figure 6. Positive periodic solutions when $\mathcal{R}_0 = 6.97762 > 1$, given the specific parameter values specified in Table 2 (persistence).

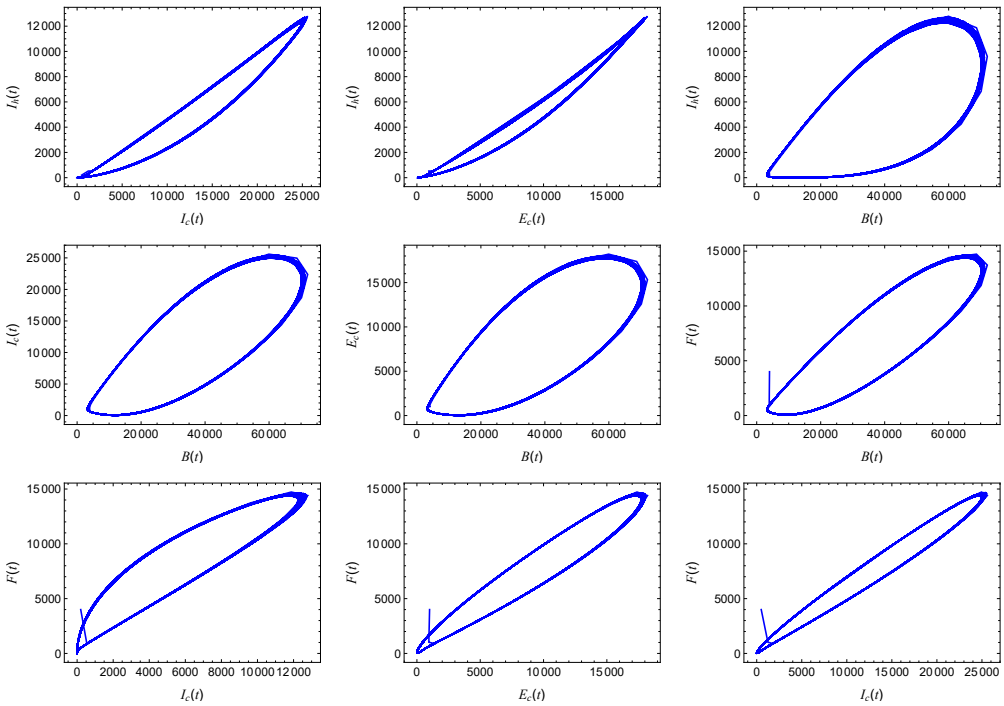

Figure 7. Positive periodic solutions when $\mathcal{R}_0 = 6.97762 > 1$, given the specific parameter values specified in Table 2 (persistence).

5.3. Sensitivity Analysis and the Impacts of Environments and Contaminated Food Products

Understanding the impact of parameter uncertainty on model predictions is a crucial aspect of sensitivity analysis [35]. This method examines how changes in parameters influence the behavior of the system, providing insights into the relationships between

parameters and outputs. By highlighting the most influential parameters, sensitivity analysis helps prioritize those that significantly affect model variability. A standard method in sensitivity analysis is to calculate sensitivity indices, which measure how changes in parameters influence outcomes [36]. The normalized forward sensitivity index, defined as $\frac{\partial v}{\partial u} \times \frac{u}{v}$, quantifies the proportional impact of a parameter (u) on a variable (v), allowing precise comparisons in differentiable systems.

Estimation of the basic reproduction number averaged in time $[\mathcal{R}_0]$ for Model (1) was based on the methodology described in [37]. To simplify the analysis, the time-dependent transmission rates $\beta_{bh}(t)$, $\beta_{bc}(t)$, and $\beta_f(t)$ were replaced with their respective time-averaged values, $[\beta_{bh}]$, $[\beta_{bc}]$, and $[\beta_f]$, for $t \geq 0$. Using these averaged parameters, the results from [37] were applied to derive $[\mathcal{R}_0]$, as detailed below.

$$[\mathcal{R}_0] = \frac{\sqrt{l_3^2 l_1^2 + 2 l_2 l_1 \left(2\alpha_h [\beta_{bc}][\beta_f]\eta\mu_b/\mu_f + \alpha_c[\beta_{bc}](\alpha_h[\beta_{bh}] - \beta_h\mu_b) - \beta_c\mu_b l_4\right)\mu_h\Pi_c + l_4^2 l_2^2}}{2\mu_b\mu_c\mu_h l_2 l_1} + \frac{l_1 l_3 + l_4 l_2}{2\mu_b\mu_c\mu_h l_2 l_1}, \tag{24}$$

where $l_1 = \gamma_h + \delta_h + \mu_h$, $l_2 = \gamma_c + \delta_c + \mu_c$, $l_3 = (\alpha_c[\beta_{bc}] + \beta_c\mu_b)\mu_h\Pi_c$, $l_4 = (\alpha_h[\beta_{bh}] + \beta_h\mu_b)\mu_c\Pi_h$.

Figure 8 reveals that several parameters significantly influence the basic reproduction number $[\mathcal{R}_0]$. The key contributors include mortality rates (μ_h, μ_c), infection rates ($[\beta_{bc}]$, $[\beta_f]$, $[\beta_{bh}]$, α_h), and decay rates (μ_b, μ_f). These results underscore the critical role of precise parameter estimation in understanding disease transmission dynamics and developing effective control strategies.

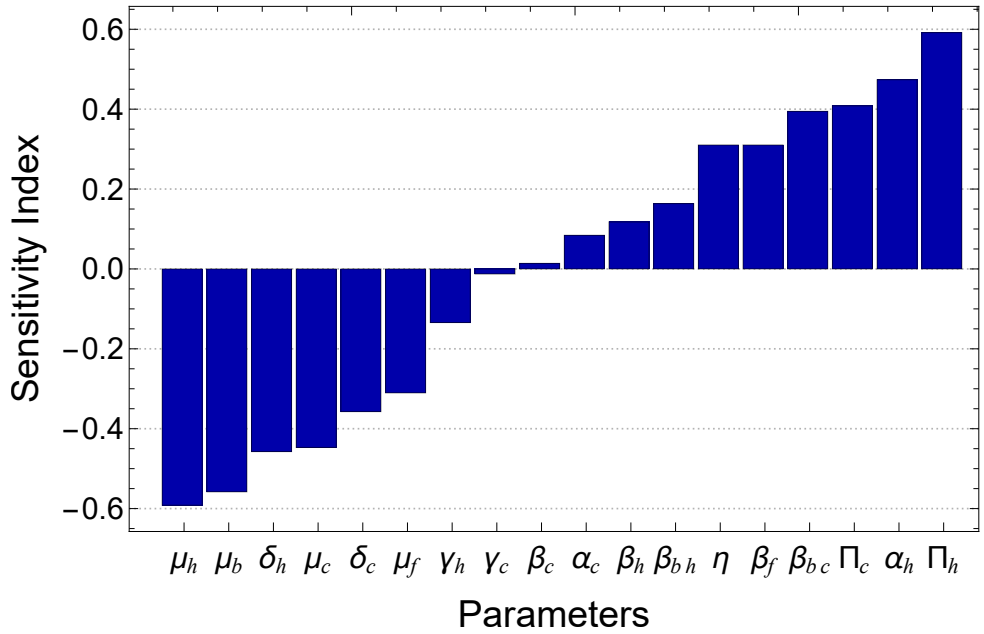

Figure 8. Sensitivity analysis for $[\mathcal{R}_0]$, using the parameter values specified in Table 2. Sensitivity indices are presented in descending order of magnitude.

We proceed to investigate how changes in key model parameters that influence contamination affect the basic reproduction number, $[\mathcal{R}_0]$. Figure 9 illustrates the behavior of $[\mathcal{R}_0]$ in response to variations in bacterial ingestion rates, the shedding rates of Salmonella by humans and cattle, the harvesting rate of contaminated food products, and the growth and decay dynamics of Salmonella.

Figure 9a illustrates the relationship between $[\mathcal{R}_0]$ and the parameters $[\beta_{bh}]$ and α_h, which represent human ingestion and shedding rates of Salmonella typhimurium bacteria. The figure highlights that $[\mathcal{R}_0]$ increases as these rates increase, underscoring their significant influence on disease transmission. These findings emphasize the sensitivity of $[\mathcal{R}_0]$ to both ingestion and shedding rates, indicating the critical need to reduce these parameters to mitigate the severity of the disease. Implementing control strategies such as the promotion of hygiene education and sanitation practices is essential to curb the shedding and ingestion of Salmonella typhimurium bacteria and reduce the potential for outbreaks.

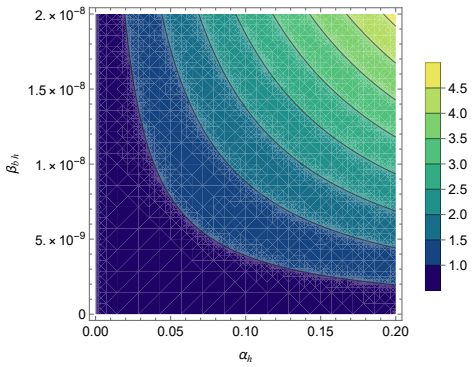

(**a**) The dynamics of $[\mathcal{R}_0]$ in relation to $[\beta_{bh}]$ and α_h.

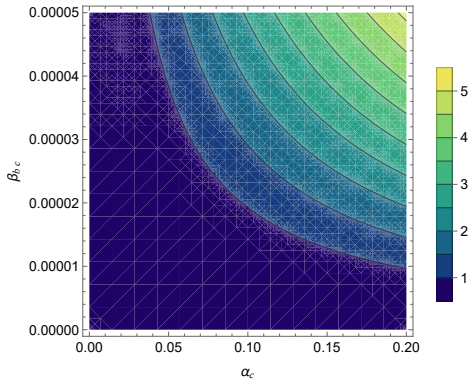

(**b**) The dynamics of $[\mathcal{R}_0]$ in relation to $[\beta_{bc}]$ and α_c.

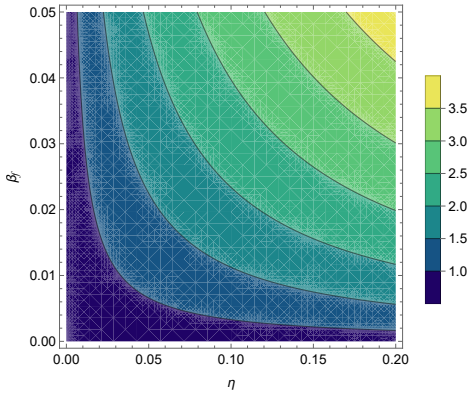

(**c**) The dynamics of $[\mathcal{R}_0]$ in relation to $[\beta_f]$ and η.

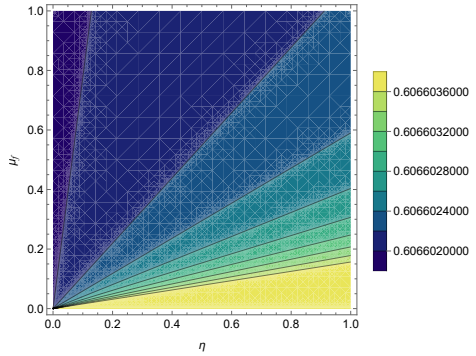

(**d**) The dynamics of $[\mathcal{R}_0]$ in relation to μ_f and η.

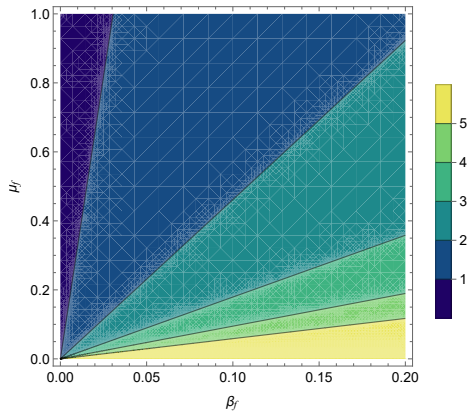

(**e**) The dynamics of $[\mathcal{R}_0]$ in relation to $[\beta_f]$ and μ_f.

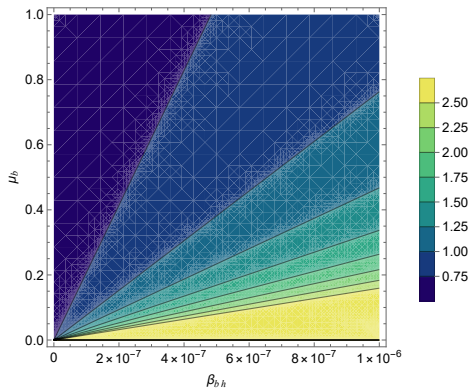

(**f**) The dynamics of $[\mathcal{R}_0]$ in relation to $[\beta_{bh}]$ and μ_b.

Figure 9. Contour plots of the time-average basic reproduction number ($[\mathcal{R}_0]$) are presented as functions of β_h, α_h, α_c, $[\beta_{bh}]$, β_c, $[\beta_{bc}]$, $[\beta_f]$, η, μ_f, and μ_b, with all other parameters set to the values given in Table 2.

Figure 9b explores $[\mathcal{R}_0]$ and the parameters $[\beta_{bc}]$ and α_c of Salmonella typhimurium in cattle. The finding indicates that higher values of these parameters significantly enhance $[\mathcal{R}_0]$, thereby facilitating the spread of the disease. This underscores the importance of controlling both rates to effectively limit the impact of salmonellosis. Implementing measures to reduce cattle exposure to contaminated environments and improving waste management practices could help to achieve this goal.

Figure 9c examines the dependence of $[\mathcal{R}_0]$ on the harvesting rate $[\beta_f]$ and η of Salmonella through food products. The figure reveals a direct relationship, where increases in either parameter lead to a rise in $[\mathcal{R}_0]$, thus amplifying the potential for secondary infections. To mitigate the risk and severity of salmonellosis, it is highly recommended to implement control measures such as the application of organic acid disinfectants to eliminate Salmonella typhimurium in food products. The relationship between $[\mathcal{R}_0]$, $[\mu_f]$, and η highlights critical factors influencing disease transmission. As depicted in Figure 9d, $[\mathcal{R}_0]$ increases when the harvesting rate increases or when the decay rate decreases, underscoring the importance of managing these parameters to control the spread of infection.

The dynamics of $[\mathcal{R}_0]$ in relation to the environmental decay rate of Salmonella typhimurium (μ_b) and the human ingestion rate ($[\beta_{bh}]$) reveal contrasting effects on the spread of the disease, as shown in Figure 9f. As the ingestion rate increases, $[\mathcal{R}_0]$ increases proportionally, indicating a higher transmission potential. In contrast, an increase in the rate of bacterial decay leads to a reduction in $[\mathcal{R}_0]$, highlighting its mitigating impact on secondary infections. Similarly, when examining $[\mathcal{R}_0]$ against the food-based parameters μ_f (decay rate) and $[\beta_f]$ (ingestion rate), Salmonella typhimurium ingestion through contaminated food products emerges as a significant driver of disease spread, reinforcing the need for strategies targeting both environmental and food-borne pathways, as shown in Figure 9e.

5.4. Model Prediction of the Future Salmonella Cases in Saudi Arabia

This study aimed to explore how changes in key parameters could contribute to an increase in Salmonella infections, potentially leading to a future epidemic in Saudi Arabia. Given the large number of parameters involved, performing a comprehensive analysis to identify the most influential factors is a complex task. Therefore, this study focuses on illustrating possible parameter variations through three specific scenarios, as shown in Figure 10.

In Figure 10, we estimate the potential impact of changes in critical parameters, including bacteria on human transmission rates ($[\beta_{bh}]$ and $[\beta_f]$), the transmission of bacteria to cattle and the transmission between cattle ($[\beta_{bc}]$ and β_c), and the rates of bacterial decay (μ_b and μ_f), on the progression of a Salmonella epidemic in Saudi Arabia. Our simulations indicate that increases in any of these parameters, whether through direct or indirect transmission, could lead to a significant increase or decrease in the number of infections. Furthermore, such changes can trigger the onset of periodic annual epidemics, marked by the recurrent appearance of Salmonella cases. These findings emphasize the need for vigilant monitoring and proactive management of these factors to prevent and control potential Salmonella outbreaks in Saudi Arabia.

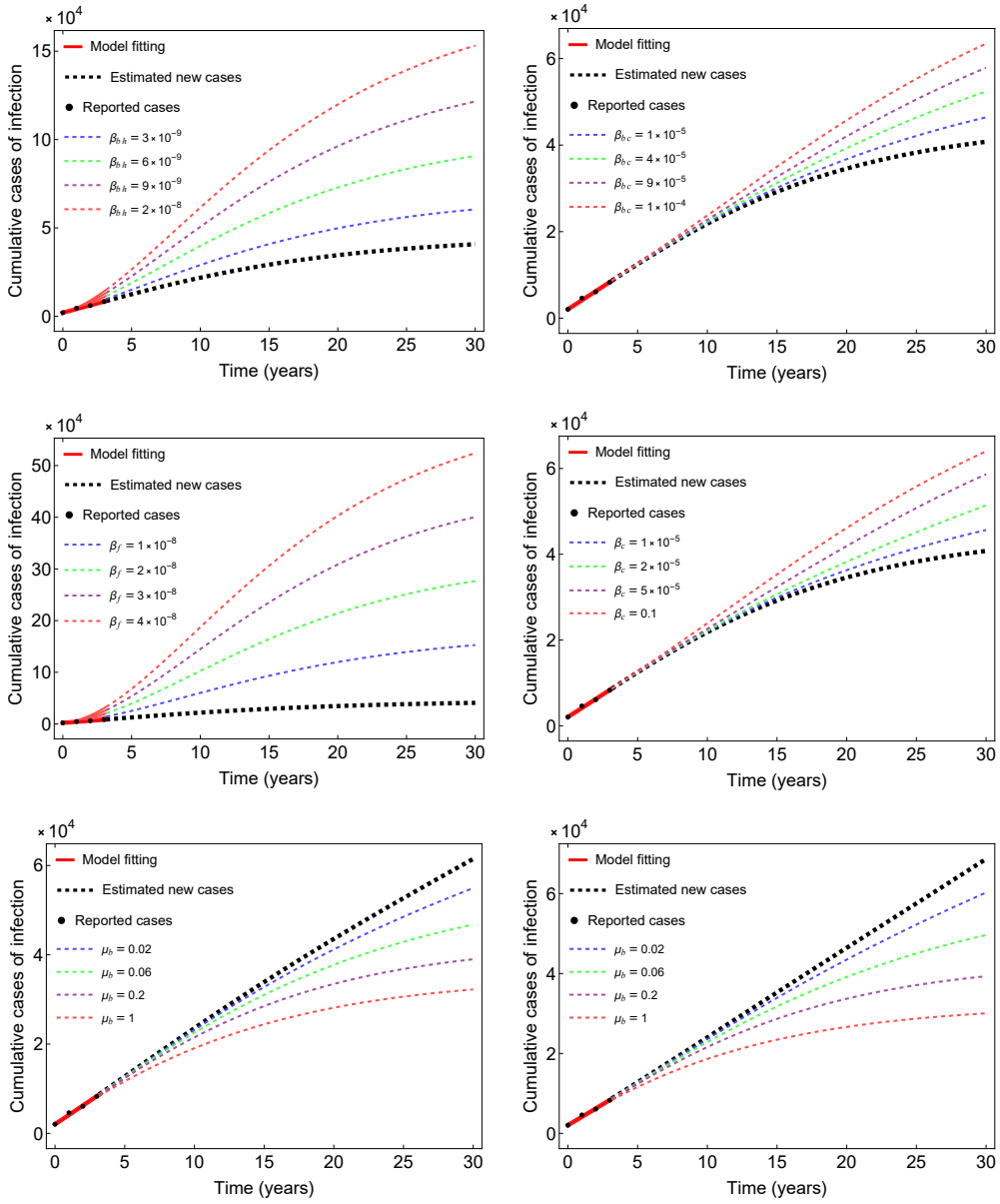

Figure 10. Prediction of new Salmonella infections in Saudi Arabia.

6. Discussion

This study provides a comprehensive analysis of the dynamics of Salmonella typhimurium transmission within human, cattle, and environmental compartments, with a particular focus on the impacts of seasonal variations, contamination through food products, and key parameters that influence disease transmission. By incorporating both analytical and numerical methods, we examine the conditions for disease extinction and persistence, sensitivity analysis, and model predictions for future Salmonella outbreaks in Saudi Arabia.

The results of our seasonal model indicate that the basic reproduction number, $\mathcal{R}_0$, plays a pivotal role in determining the long-term dynamics of Salmonella infections. Specifically, when $\mathcal{R}_0 < 1$, the disease-free equilibrium is globally stable, leading to the extinction of the pathogen from the population, as demonstrated in Theorem 3 and Figure 4. This finding is consistent with previous research that indicates that $\mathcal{R}_0$ serves as a crucial threshold parameter for understanding the dynamics of infectious diseases, including Salmonella. In contrast, when $\mathcal{R}_0 > 1$, persistent infection dynamics emerge, characterized by periodic outbreaks and the maintenance of Salmonella within the population, as shown in Theorem 4 and Figures 5–7. These findings underscore the importance of maintaining

$\mathcal{R}_0$ below the threshold through targeted interventions, such as improved sanitation, vaccination, and public health measures, to mitigate the risk of endemic transmission and prevent recurrent outbreaks of Salmonella. Figure 2 presents the dynamics captured by the model for the outbreak of Salmonella in Saudi Arabia between 2018 and 2021, together with a good fit for both cumulative and newly infected cases. The key parameters, summarized in Table 2, yield a basic reproduction number ($\mathcal{R}_0 \approx 0.606602$), indicating that transmission is not sustainable and will eventually decay. This is further supported by the projections in Figure 3, which show new cases gradually falling to almost zero within these few years and leveling out at around 40,000 cumulative cases. However, it is important to note that the data fitting is based on a limited dataset spanning only a few years (2018–2021), which poses a significant limitation to the analysis. The restricted temporal scope may not fully capture the long-term dynamics or potential seasonal variations in Salmonella transmission, potentially affecting the accuracy of the model's predictions. Future studies should aim to incorporate more extensive datasets to improve the robustness and reliability of the findings.

The sensitivity analysis conducted in this study reveals that various parameters, particularly those related to bacterial shedding rates (β_{bh}, β_{bc}, human ingestion rates, and the decay rates of Salmonella in the environment and food, significantly influence the basic reproduction number. This highlights the critical role of precise parameter estimation in understanding disease transmission dynamics. The results suggest that intervention strategies targeting both human and animal transmission routes, such as improved hygiene practices, sanitation, and control of bacterial contamination in food products, could be pivotal in reducing Salmonella transmission. In addition, sensitivity indices indicate that mortality rates (μ_h, μ_c) and bacterial growth and decay parameters have a significant effect on model predictions, confirming the need to consider environmental factors in disease control strategies. Our model also provides important information on the role of foodborne and environmental transmission in Salmonella spread. The sensitivity analysis presented in Figure 9 illustrates how variations in foodborne contamination rates (β_f) and environmental decay rates (μ_b, μ_f) can alter disease dynamics. These findings suggest that controlling contamination in the food production and distribution stages, along with environmental interventions to limit bacterial persistence, is crucial to reducing the risk of Salmonella outbreaks. The results also emphasize the need for a multifaceted approach to controlling disease, involving both direct interventions (e.g., improved sanitation) and indirect measures (e.g., controlling environmental contamination).

Furthermore, predictions for future Salmonella infections in Saudi Arabia, as presented in Figure 10, provide valuable information on how changes in key parameters could potentially trigger future epidemics. Our simulations indicate that increases in parameters related to transmission rates, such as bacterial ingestion rates by humans and cattle, as well as bacterial shedding rates, could significantly increase the number of infections, leading to periodic outbreaks. This highlights the importance of continuous monitoring and proactive intervention strategies to prevent large-scale epidemics.

In conclusion, this study emphasizes the complex dynamics of Salmonella transmission and the influence of key parameters on its persistence in human, cattle, and environmental compartments, including contaminated environments and food products. Although the model offers valuable predictions for future outbreaks, its accuracy is dependent on precise parameter estimates, highlighting the need for further empirical data and model calibration. The findings underscore the importance of integrated control strategies targeting human and cattle reservoirs, as well as contaminated environments and food products, with the model serving as a useful tool to guide public health interventions and disease prevention efforts in regions with similar transmission dynamics.

Author Contributions: Conceptualization, M.H.A., F.K.A. and M.A.I.; methodology, M.H.A., F.K.A. and M.A.I.; software, M.H.A. and M.A.I.; validation, M.H.A., F.K.A. and M.A.I.; formal analysis, M.H.A. and M.A.I.; investigation, M.H.A., F.K.A. and M.A.I.; writing—original draft preparation, M.H.A., F.K.A. and M.A.I.; writing—review and editing, M.H.A., F.K.A. and M.A.I.; visualization, M.H.A., F.K.A. and M.A.I.; funding acquisition, M.H.A. All authors have read and agreed to the published version of the manuscript.

Funding: This work was funded by the University of Jeddah, Jeddah, Saudi Arabia, under grant No. (UJ-24-DR-711-1).

Data Availability Statement: The original contributions presented in this study are included in the article. Further inquiries can be directed to the corresponding authors.

Acknowledgments: Therefore, the authors thank the University of Jeddah for its technical and financial support.

Conflicts of Interest: The authors declare no conflicts of interest.

References

1. Arya, G.; Holtslander, R.; Robertson, J.; Yoshida, C.; Harris, J.; Parmley, J.; Nichani, A.; Johnson, R.; Poppe, C. Epidemiology, pathogenesis, genoserotyping, antimicrobial resistance, and prevention and control of non-typhoidal Salmonella serovars. *Curr. Clin. Microbiol. Rep.* **2017**, *4*, 43–53. [CrossRef]
2. Machado Junior, P.C.; Chung, C.; Hagerman, A. Modeling Salmonella spread in broiler production: Identifying determinants and control strategies. *Front. Vet. Sci.* **2020**, *7*, 564. [CrossRef] [PubMed]
3. Rahman, M.T.; Sobur, M.A.; Islam, M.S.; Ievy, S.; Hossain, M.J.; El Zowalaty, M.E.; Rahman, A.T.; Ashour, H.M. Zoonotic diseases: Etiology, impact, and control. *Microorganisms* **2020**, *8*, 1405. [CrossRef] [PubMed]
4. Cole, D.; Gould, L.H.; Hall, A.J.; Herman, K.; Vieira, A.R.; Walsh, K.A.; Williams, I.T. Surveillance for foodborne disease outbreaks–United States, 1998–2008. *Surveill. Summ.* **2013**, *62*, 1–34.
5. Centers for Disease Control and Prevention. Surveillance for foodborne disease outbreaks–United States, 2009–2010. *MMWR. Morb. Mortal. Wkly. Rep.* **2013**, *62*, 41–47.
6. Abd El-Ghany, W.A. Salmonellosis: A food borne zoonotic and public health disease in Egypt. *J. Infect. Dev. Ctries.* **2020**, *14*, 674–678. [CrossRef] [PubMed]
7. Majowicz, S.E.; Musto, J.; Scallan, E.; Angulo, F.J.; Kirk, M.; O'Brien, S.J.; Jones, T.F.; Fazil, A.; Hoekstra, R.M.; International Collaboration on Enteric Disease "Burden of Illness" Studies. The global burden of nontyphoidal Salmonella gastroenteritis. *Clin. Infect. Dis.* **2010**, *50*, 882–889. [CrossRef]
8. Fisman, D.N. Seasonality of infectious diseases. *Annu. Rev. Public Health* **2007**, *28*, 127–143. [CrossRef] [PubMed]
9. Humphrey, T. Salmonella, stress responses and food safety. *Nat. Rev. Microbiol.* **2004**, *2*, 504–509. [CrossRef]
10. Haley, B.J.; Cole, D.J.; Lipp, E.K. Distribution, diversity, and seasonality of waterborne salmonellae in a rural watershed. *Appl. Environ. Microbiol.* **2009**, *75*, 1248–1255. [CrossRef] [PubMed]
11. Admasu, H.N.; Bedassa, A.; Tessema, T.S.; Kovac, J.; Vipham, J.L.; Woldegiorgis, A.Z. Seasonal variation of Salmonella enterica prevalence in milk and cottage cheese along the dairy value chain in three regions of Ethiopia. *Food Saf. Risk* **2024**, *11*, 2. [CrossRef]
12. Bondo, K.J.; Pearl, D.L.; Janecko, N.; Boerlin, P.; Reid-Smith, R.J.; Parmley, J.; Jardine, C.M. Impact of season, demographic and environmental factors on Salmonella occurrence in raccoons (Procyon lotor) from swine farms and conservation areas in southern Ontario. *PLoS ONE* **2016**, *11*, e0161497. [CrossRef] [PubMed]
13. Martinez-Urtaza, J.; Liebana, E. Investigation of clonal distribution and persistence of Salmonella Senftenberg in the marine environment and identification of potential sources of contamination. *FEMS Microbiol. Ecol.* **2005**, *52*, 255–263. [CrossRef] [PubMed]
14. Oludairo, O.O.; Kwaga, J.K.; Kabir, J.; Abdu, P.A.; Gitanjali, A.; Perrets, A.; Cibin, V.; Lettini, A.A.; Aiyedun, J.O. Ecology and epidemiology of Salmonella spp. isolated from the environment and the roles played by wild animals in their maintenance. *Int. J. One Health* **2023**, *9*, 1–9. [CrossRef]
15. Roshdy, H.; Mohamed, S.; Elsebaey, H.; El-Demerdash, G. Effect of Age and Season on Salmonella Infection in Broiler Chickens with Special Reference to Virulence and Antibiotic Resistance Genes. *Zagazig Vet. J.* **2020**, *48*, 328–339.
16. Pérez, J.; Contreras-Moreno, F.J.; Marcos-Torres, F.J.; Moraleda-Muñoz, A.; Muñoz-Dorado, J. The antibiotic crisis: How bacterial predators can help. *Comput. Struct. Biotechnol. J.* **2020**, *18*, 2547–2555. [CrossRef] [PubMed]
17. Qin, L.; Yang, S.X.; Meng, M.Q.H. A mathematical model with degree of risk for Salmonella infections. In Proceedings of the 2007 IEEE International Conference on Systems, Man and Cybernetics, Montreal, QC, Canada, 7–10 October 2007; pp. 2704–2709.

18. Collineau, L.; Phillips, C.; Chapman, B.; Agunos, A.; Carson, C.; Fazil, A.; Reid-Smith, R.J.; Smith, B.A. A within-flock model of Salmonella Heidelberg transmission in broiler chickens. *Prev. Vet. Med.* **2020**, *174*, 104823. [CrossRef] [PubMed]
19. Trazias, H.; Irunde, J.I.; Kgosimore, M.; Mayengo, M.M. Dynamics of Salmonellosis and the impacts of contaminated dairy products and environments: Mathematical modeling perspective and parameter estimation. *Ecol. Model.* **2024**, *497*, 110862. [CrossRef]
20. Nyerere, N.; Luboobi, L.S.; Mpeshe, S.C.; Shirima, G.M. Modeling the impact of seasonal weather variations on the infectiology of brucellosis. *Comput. Math. Methods Med.* **2020**, *2020*, 8972063. [CrossRef] [PubMed]
21. Naumova, E.N.; Jagai, J.S.; Matyas, B.; DeMaria, A.; MacNeill, I.; Griffiths, J. Seasonality in six enterically transmitted diseases and ambient temperature. *Epidemiol. Infect.* **2007**, *135*, 281–292. [CrossRef]
22. Rushton, S.P.; Sanderson, R.A.; Diggle, P.J.; Shirley, M.D.; Blain, A.P.; Lake, I.; Maas, J.A.; Reid, W.D.; Hardstaff, J.; Williams, N.; et al. Climate, human behaviour or environment: Individual-based modelling of Campylobacter seasonality and strategies to reduce disease burden. *J. Transl. Med.* **2019**, *17*, 34. [CrossRef]
23. Simpson, R.B.; Zhou, B.; Naumova, E.N. Seasonal synchronization of foodborne outbreaks in the United States, 1996–2017. *Sci. Rep.* **2020**, *10*, 17500. [CrossRef]
24. Smith, H.L. *Monotone Dynamical Systems: An Introduction to the Theory of Competitive and Cooperative Systems: An Introduction to the Theory of Competitive and Cooperative Systems*; Number 41; American Mathematical Society: Providence, RI, USA, 1995.
25. Wang, W.; Zhao, X.Q. Threshold dynamics for compartmental epidemic models in periodic environments. *J. Dyn. Differ. Equ.* **2008**, *20*, 699–717. [CrossRef]
26. Zhang, F.; Zhao, X.Q. A periodic epidemic model in a patchy environment. *J. Math. Anal. Appl.* **2007**, *325*, 496–516. [CrossRef]
27. Tian, J.P.; Wang, J. Some results in Floquet theory, with application to periodic epidemic models. *Appl. Anal.* **2015**, *94*, 1128–1152. [CrossRef]
28. Rebelo, C.; Margheri, A.; Bacaër, N. Persistence in seasonally forced epidemiological models. *J. Math. Biol.* **2011**, *64*, 933–949. [CrossRef] [PubMed]
29. Smith, H.L.; Waltman, P. *The Theory of the Chemostat: Dynamics of Microbial Competition*; Cambridge University Press: Cambridge, UK, 1995.
30. Zhao, X.Q. *Dynamical Systems in Population Biology*; Springer: Berlin/Heidelberg, Germany, 2003.
31. Alhumaid, N.K.; Alajmi, A.M.; Alosaimi, N.F.; Alotaibi, M.; Almangour, T.A.; Nassar, M.S.; Memish, Z.A.; Binjomah, A.Z.; Al-Jedai, A.; Almutairi, A.S.; et al. Epidemiology of Reportable Bacterial Infectious Diseases in Saudi Arabia. *Infect. Dis. Ther.* **2024**, *13*, 667–684. [CrossRef]
32. McKay, M.D.; Beckman, R.J.; Conover, W.J. Comparison of three methods for selecting values of input variables in the analysis of output from a computer code. *Technometrics* **1979**, *21*, 239–245.
33. The World Bank. Saudi Arabia–Health. 2021. Available online: https://data.worldbank.org/country/saudi-arabia (accessed on 1 November 2024).
34. Mitchell, C.; Kribs, C. A comparison of methods for calculating the basic reproductive number for periodic epidemic systems. *Bull. Math. Biol.* **2017**, *79*, 1846–1869. [CrossRef] [PubMed]
35. Saltelli, A. Sensitivity analysis for importance assessment. *Risk Anal.* **2002**, *22*, 579–590. [CrossRef] [PubMed]
36. Arriola, L.; Hyman, J.M. Sensitivity analysis for uncertainty quantification in mathematical models. In *Mathematical and Statistical Estimation Approaches in Epidemiology*; Springer: Dordrecht, The Netherlands, 2009; pp. 195–247.
37. Van den Driessche, P.; Watmough, J. Reproduction numbers and sub-threshold endemic equilibria for compartmental models of disease transmission. *Math. Biosci.* **2002**, *180*, 29–48. [CrossRef] [PubMed]

Disclaimer/Publisher's Note: The statements, opinions and data contained in all publications are solely those of the individual author(s) and contributor(s) and not of MDPI and/or the editor(s). MDPI and/or the editor(s) disclaim responsibility for any injury to people or property resulting from any ideas, methods, instructions or products referred to in the content.